Rupture risk estimation in thoracic aortic aneurysms

Prof Stéphane AVRIL (avril@emse.fr)

Where do I come from?

Demanget et al., Perrin et al.

MINES SAINT-ETIENNE
First Grande Ecole outside Paris
Founded in 1816

CHU Saint-Étienne

UNIVERSITÉ DE LYON

MINES Saint-Étienne

SAINBIOSE
SAnté INgéniérie BIOlogie Saint-Etienne
U1059 • INSERM • SAINT-ETIENNE

Inserm
Institut national de la santé et de la recherche médicale

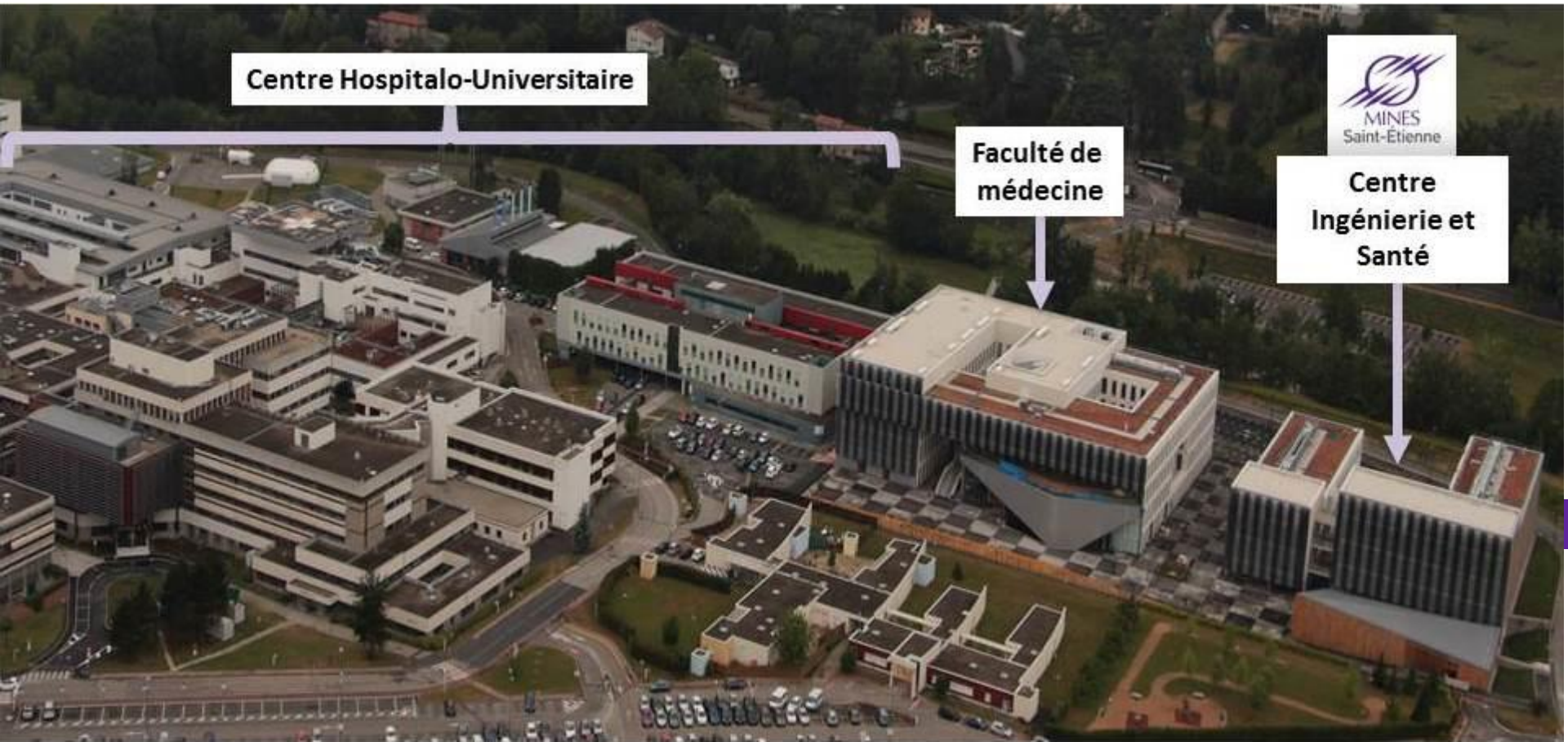

Biomechanics of soft tissues at different scales

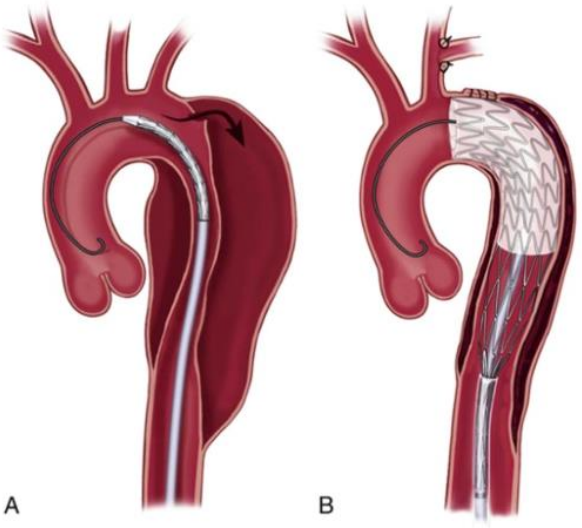

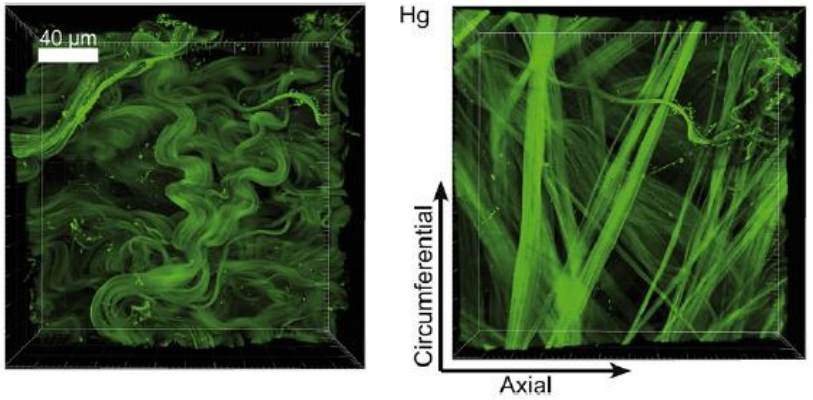

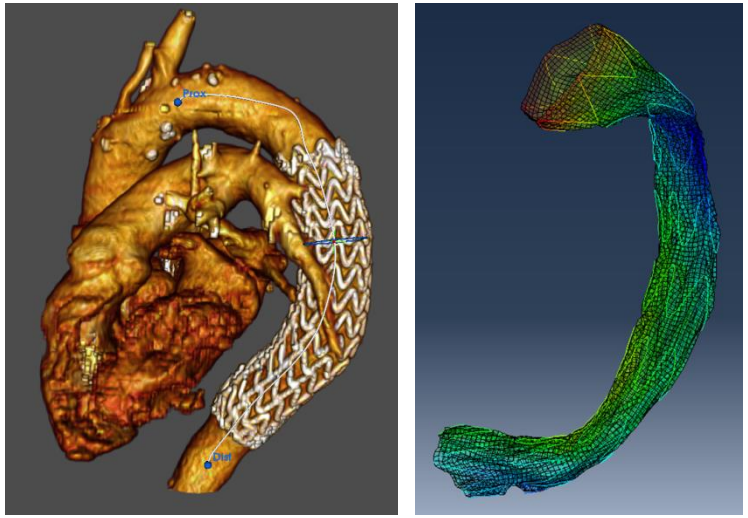

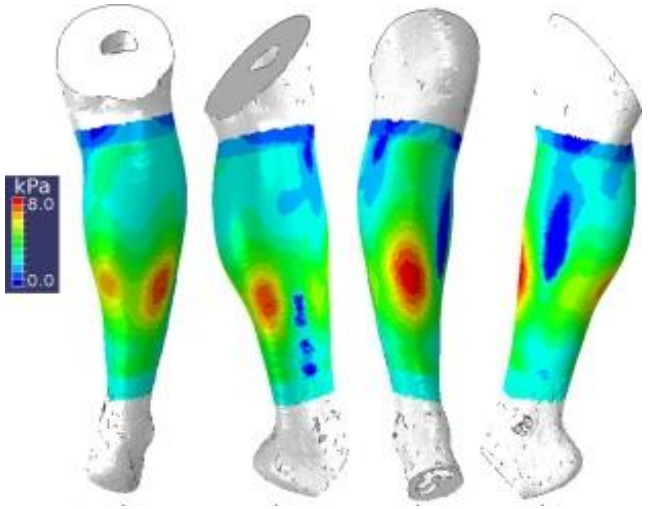

What is an ATAA and why is serious?

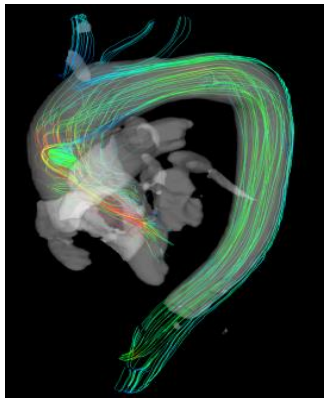

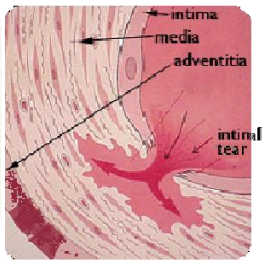

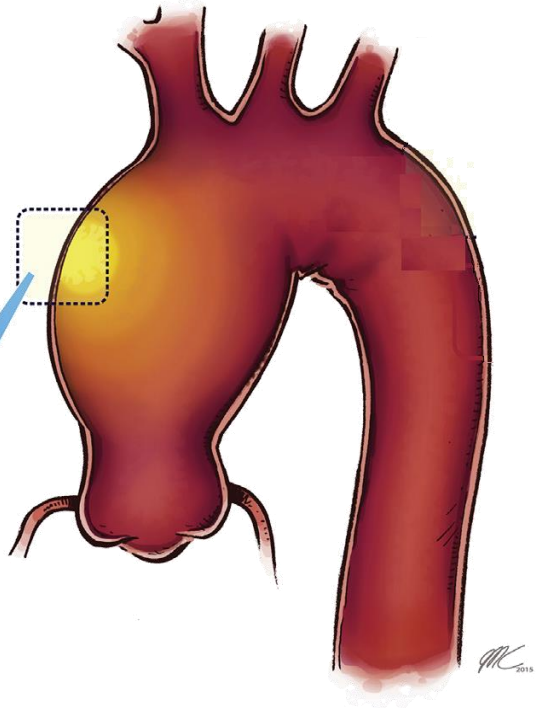

dissection

avril@emse.fr

Epidemiology statistics

Incidence : 10.4 per 100 000 persons

Elevated mortality without treatment for acute aortic dissection:
50% in 48 hours / 90% in 3 months

BAV patients: ½ develops an ATAA

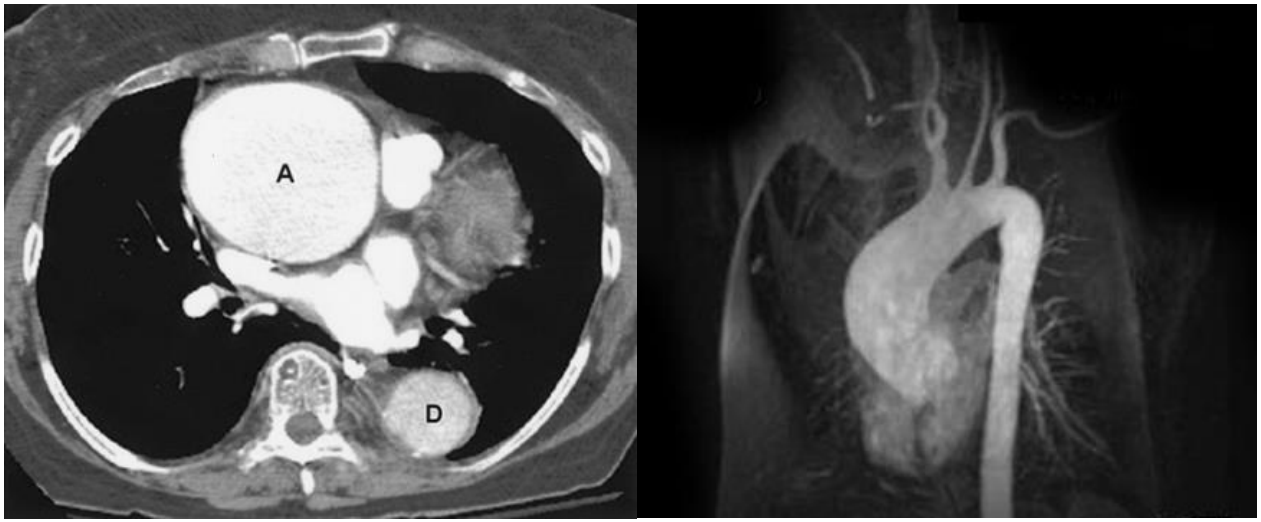

Risk management

Decision of surgical repair based on a measure if the Maximal Diameter

- **The International Registry of Acute Aortic Dissection (IRAD): among 591 type A aortic dissection, 59% had a diameter <5.5 cm (Pape, 2007)**

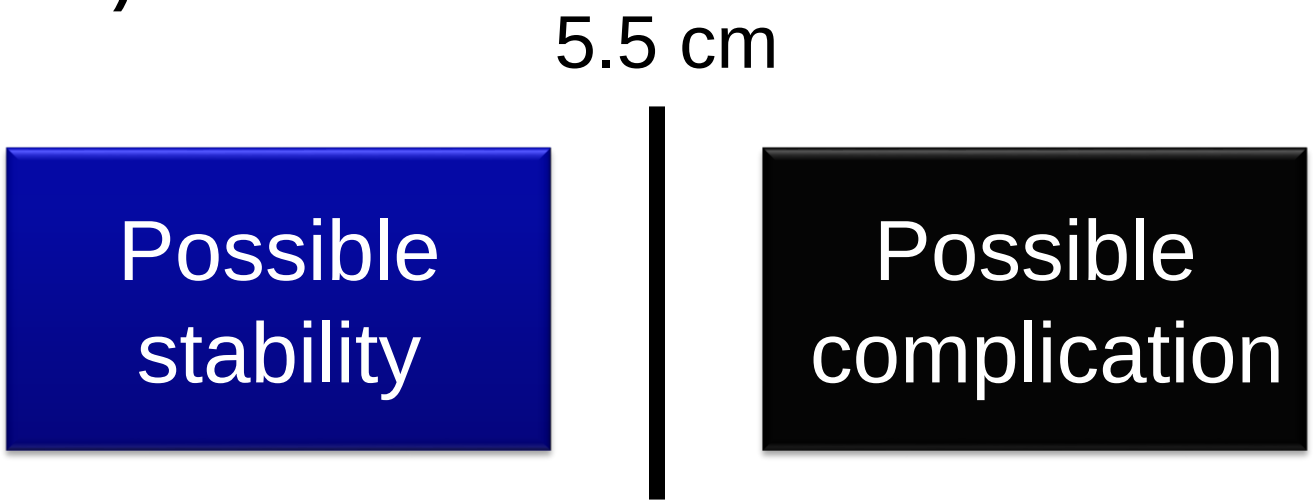

Pape et al, *Aortic Diameter ≥5.5 cm Is Not a Good Predictor of Type A Aortic Dissection Observations From the International Registry of Acute Aortic Dissection (IRAD)*, Circulation, 2007

Added value of biomechanics

- **New insights on aneurysm rupture mechanisms**
  - Arterial wall mechanics
  - How does it rupture ?
  - When ?

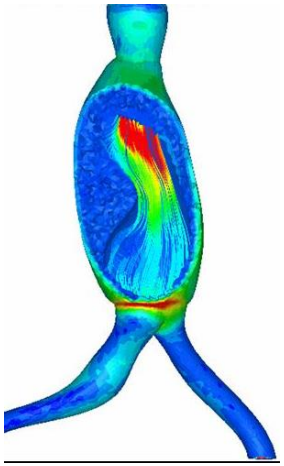

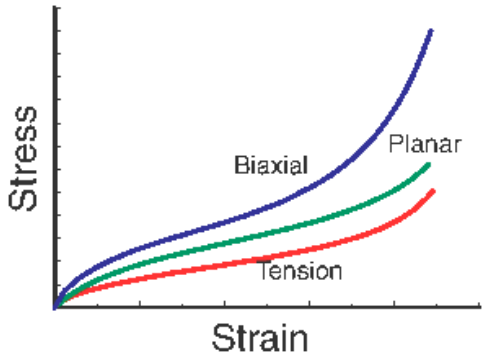

Scotti, 2007

- **New patient-specific decision making tool**
  - Patient-specific
  - From medical images

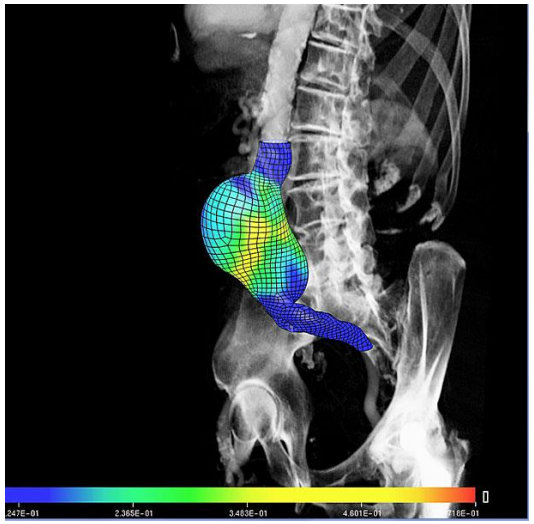

Vascops

avril@emse.fr

Recent developments in computational modeling and challenges

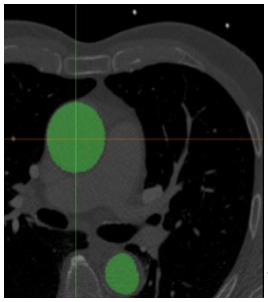

O. Trabelsi, et al, Patient specific stress and rupture analysis of ascending thoracic aneurysms, J. Biomech. (2015).
G. Martufi, et al, Is There a Role for Biomechanical Engineering in Helping to Elucidate the Risk Profile of the Thoracic Aorta?, Ann. Thorac. Surg. 101 (2016) 390–398.
S. Pasta et al., Constitutive modeling of ascending thoracic aortic aneurysms using microstructural parameters, Med. Eng. Phys. 38 (2016) 121–130.

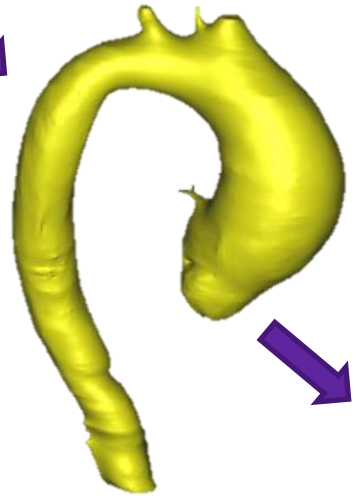

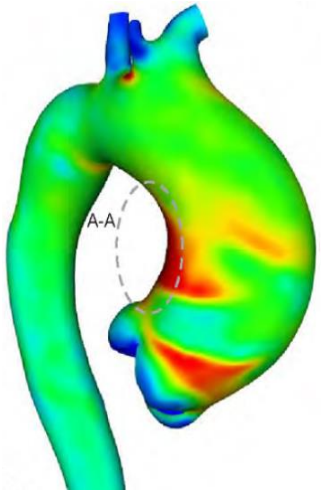

Finite-element modeling

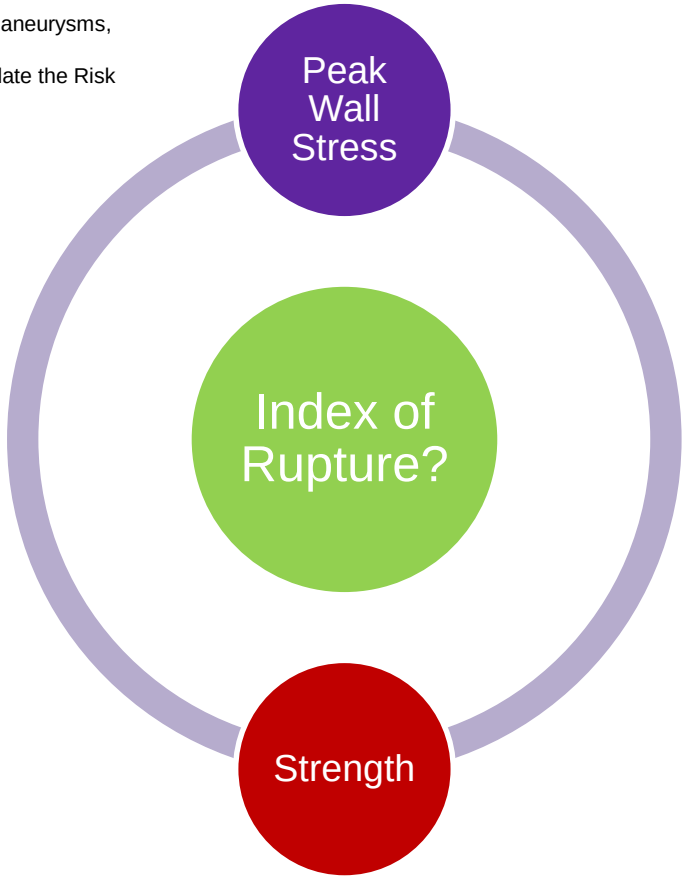

SAINT-ETIENNE PROTOCOL

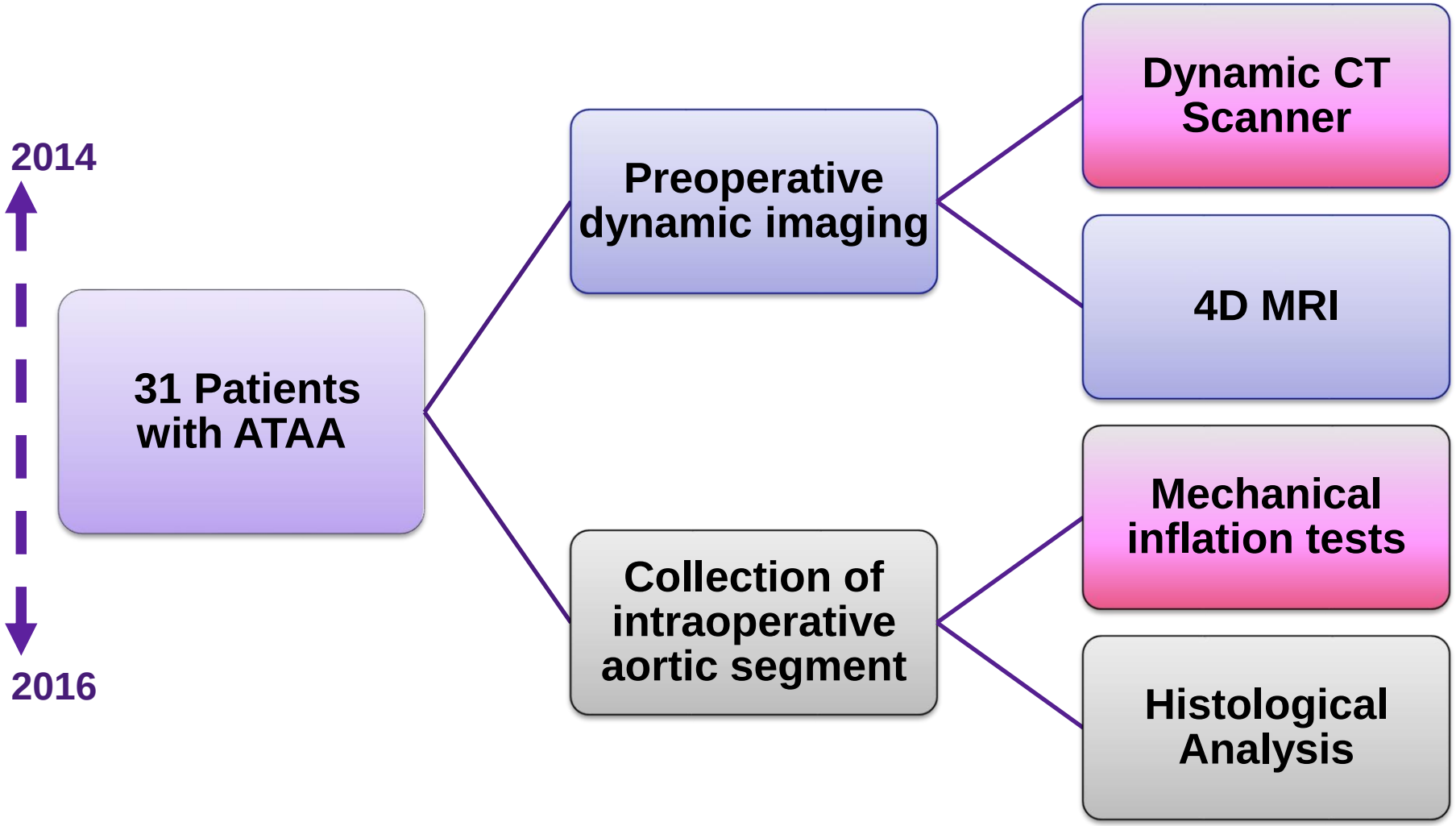

Bulge inflation tests

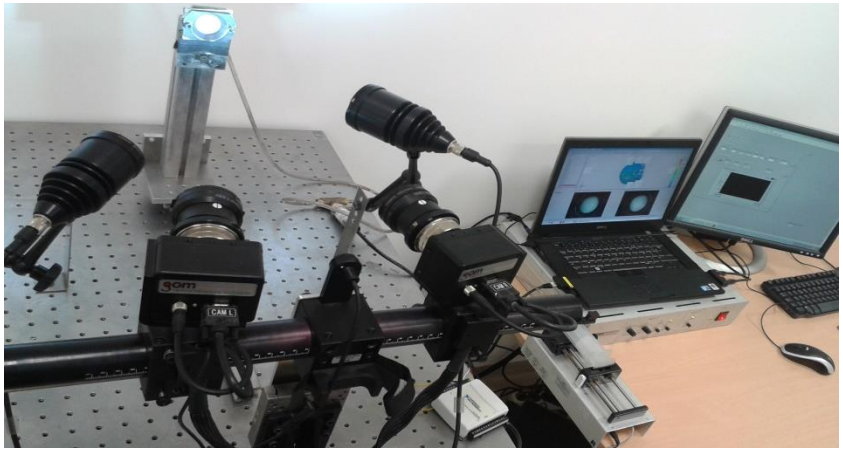

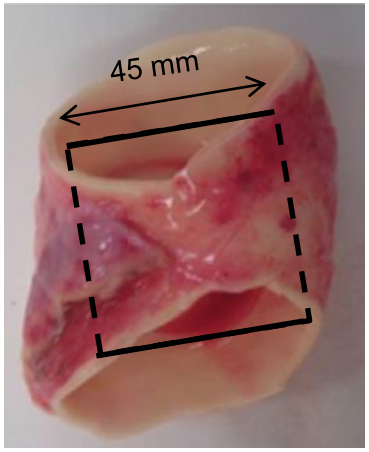

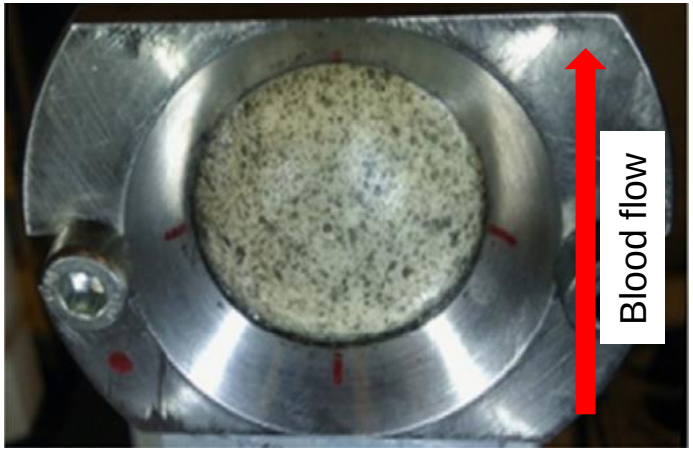

Inverse membrane analysis + digital image correlation ⇒ stress & strain reconstruction.
⇒biaxial failure properties

Trabelsi, O., Davis, F.M., Rodriguez-Matas, J.F., Duprey, A., Avril, S. Patient specific stress and rupture analysis of ascending thoracic aneurysms. Journal of Biomechanics, 2015.

Collection of the samples

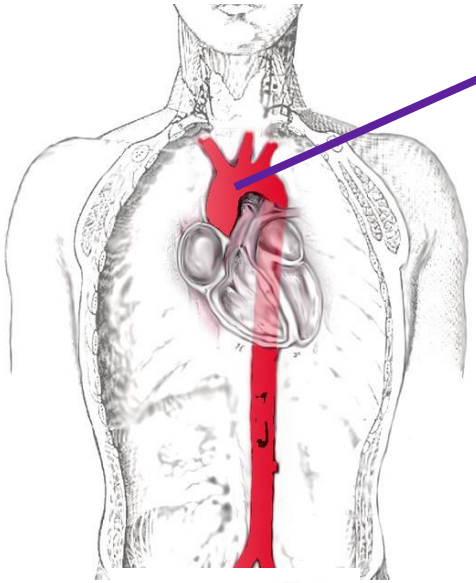

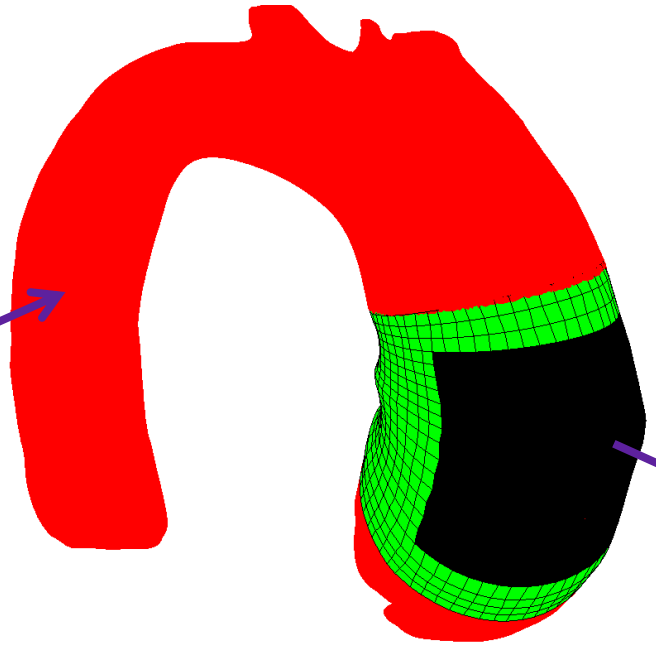

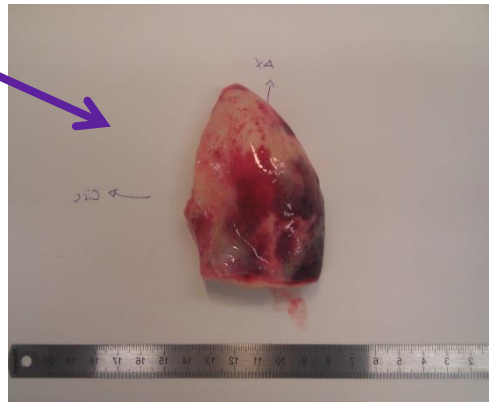

CHU Saint-Étienne

PREPARATION

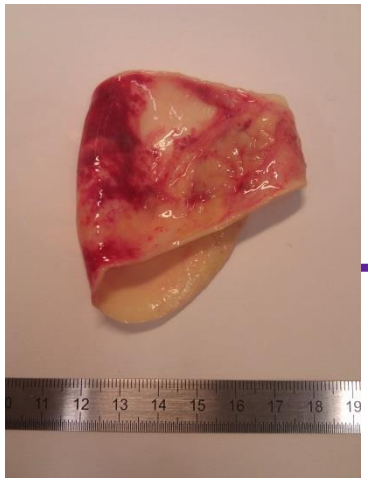

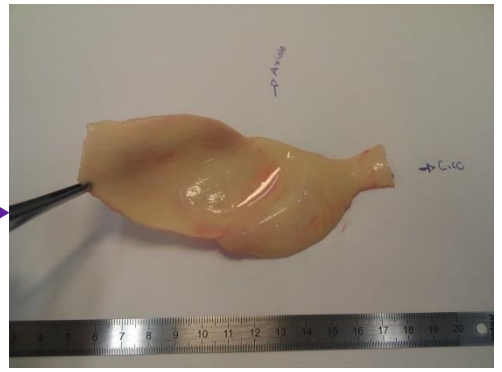

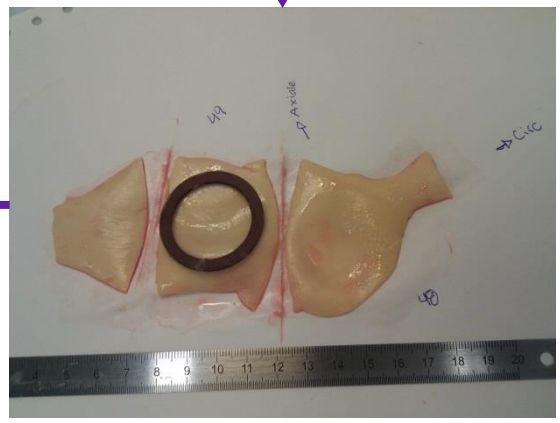

avril@emse.fr

MINES Saint-Étienne

Bulge inflation test

Romo et al. Journal of Biomechanics -2014.

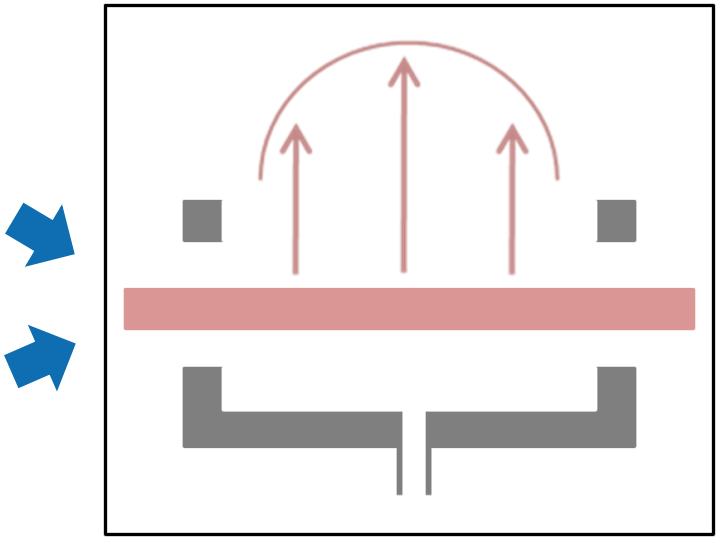

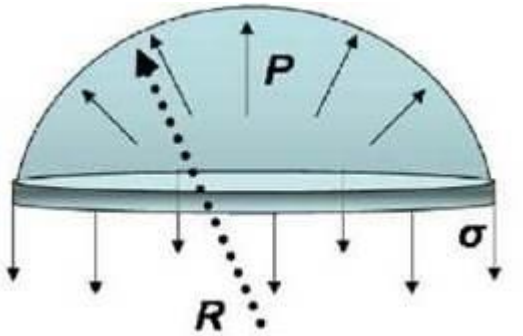

Rupture profiles

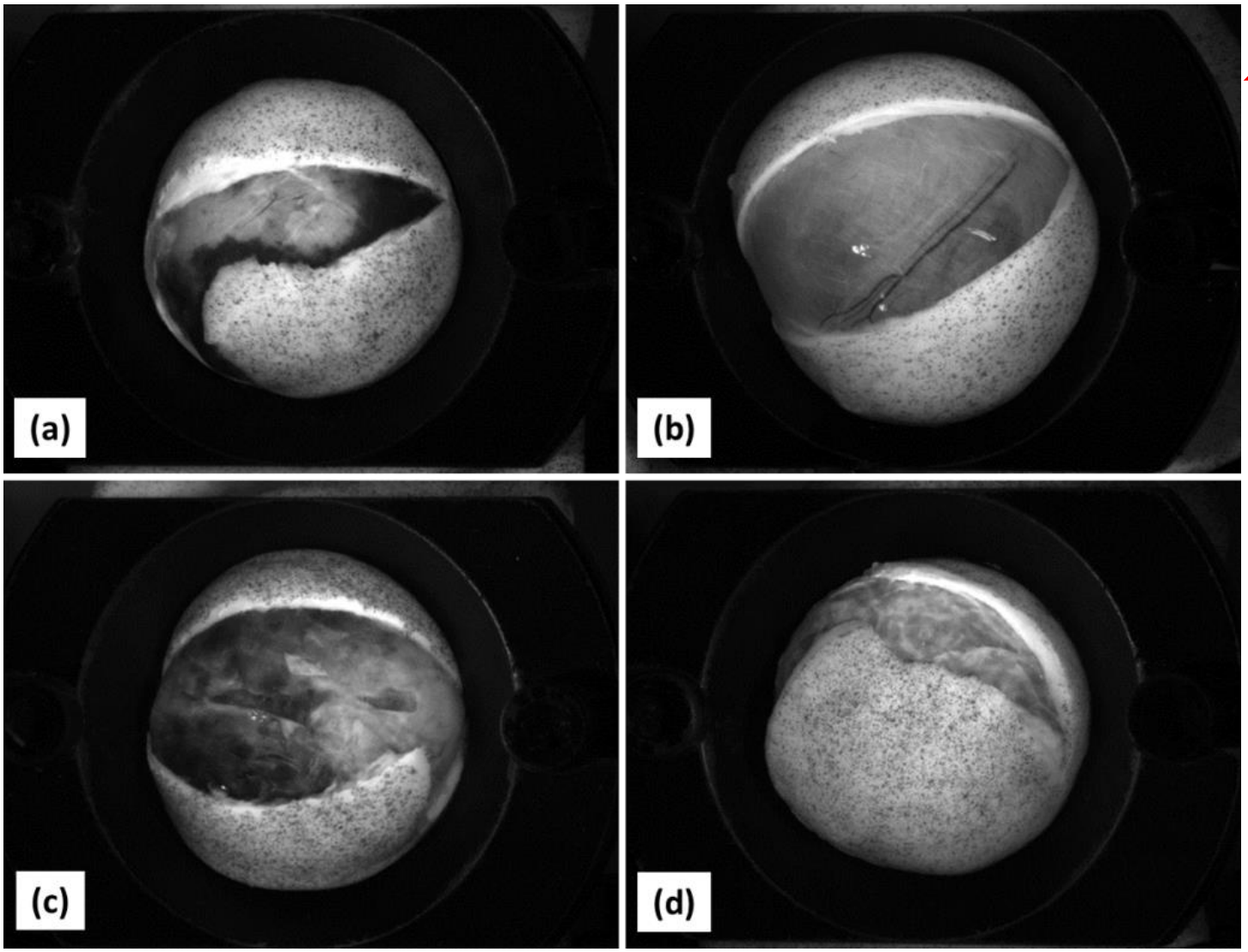

Blood flow

50% of aortas ruptured with an angle θ equal to 90 °

Full-field measurements using sDIC

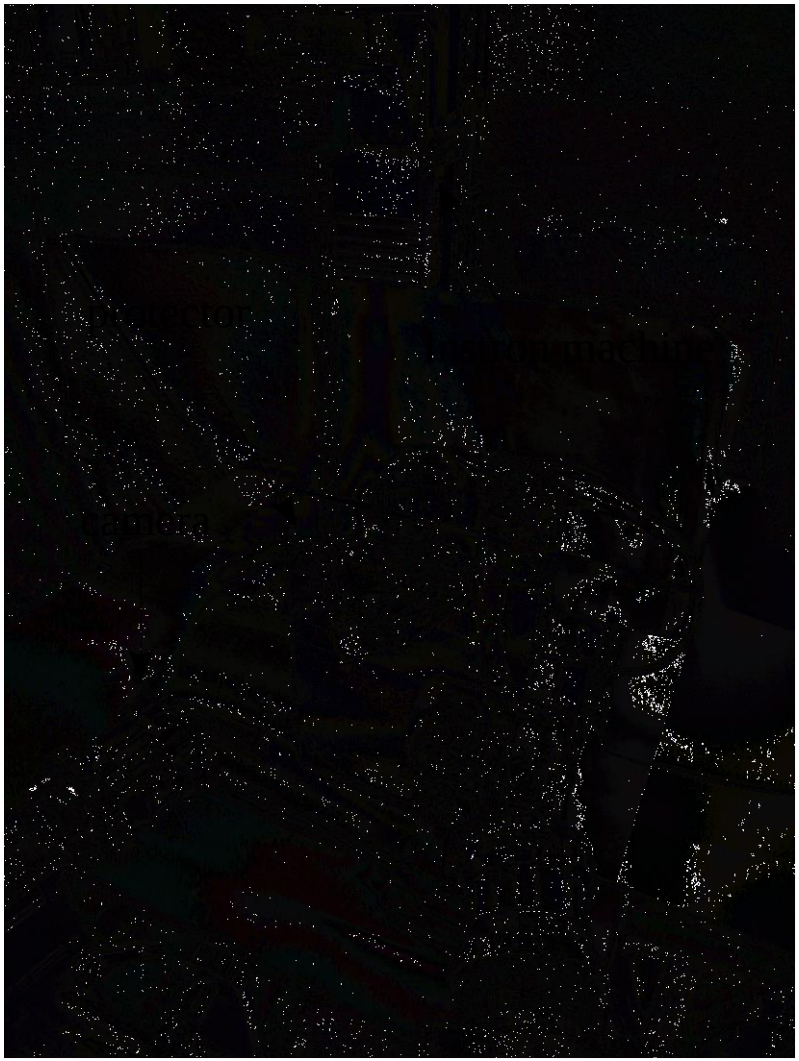

Undeformed

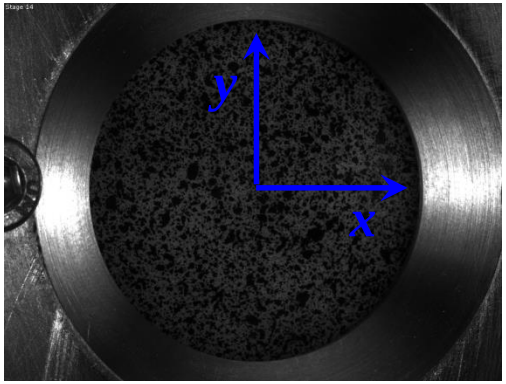

Deformed

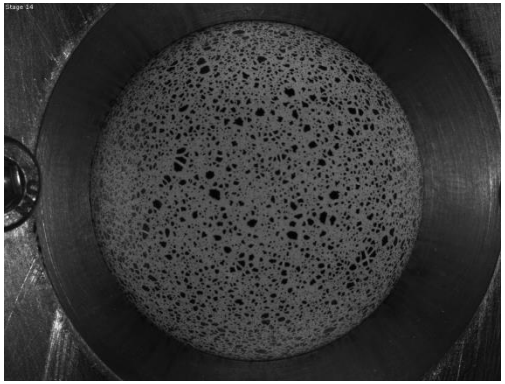

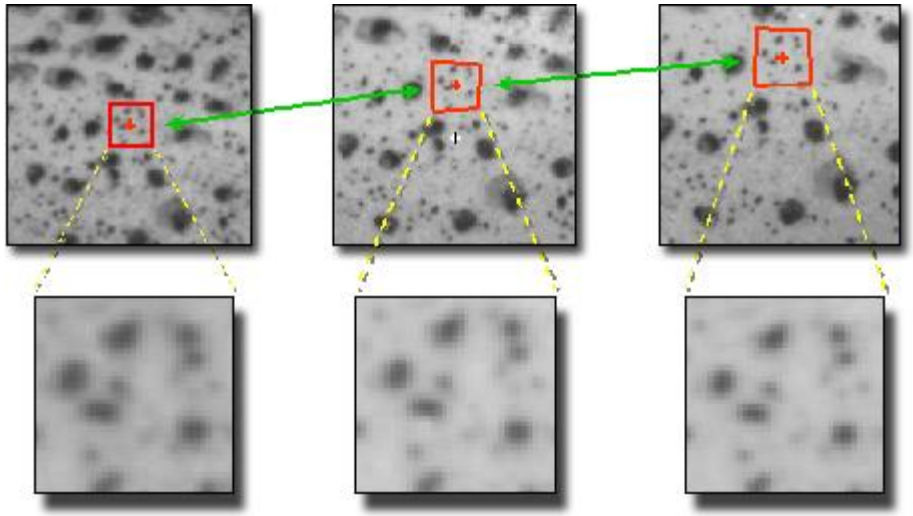

Local stress reconstruction

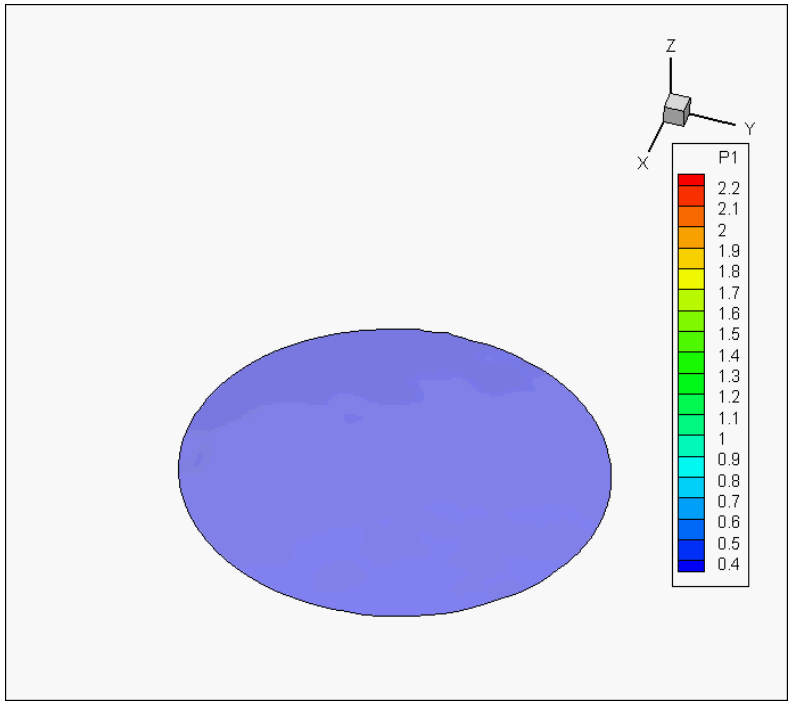

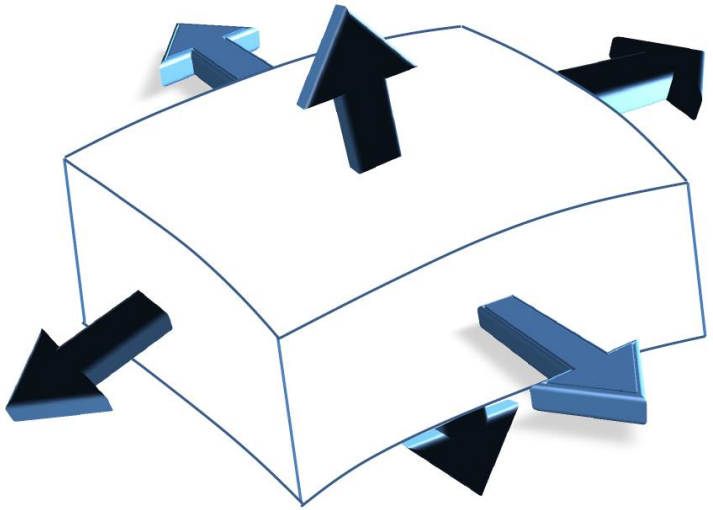

$$div(\boldsymbol{\sigma}) + f = 0$$

$$[A] \cdot [\boldsymbol{\sigma}] = [B]$$

avril@emse.fr

Stress strain analysis in the bulge test

σ_{rup} : Rupture stress, λ_{rup} : Rupture stretch,

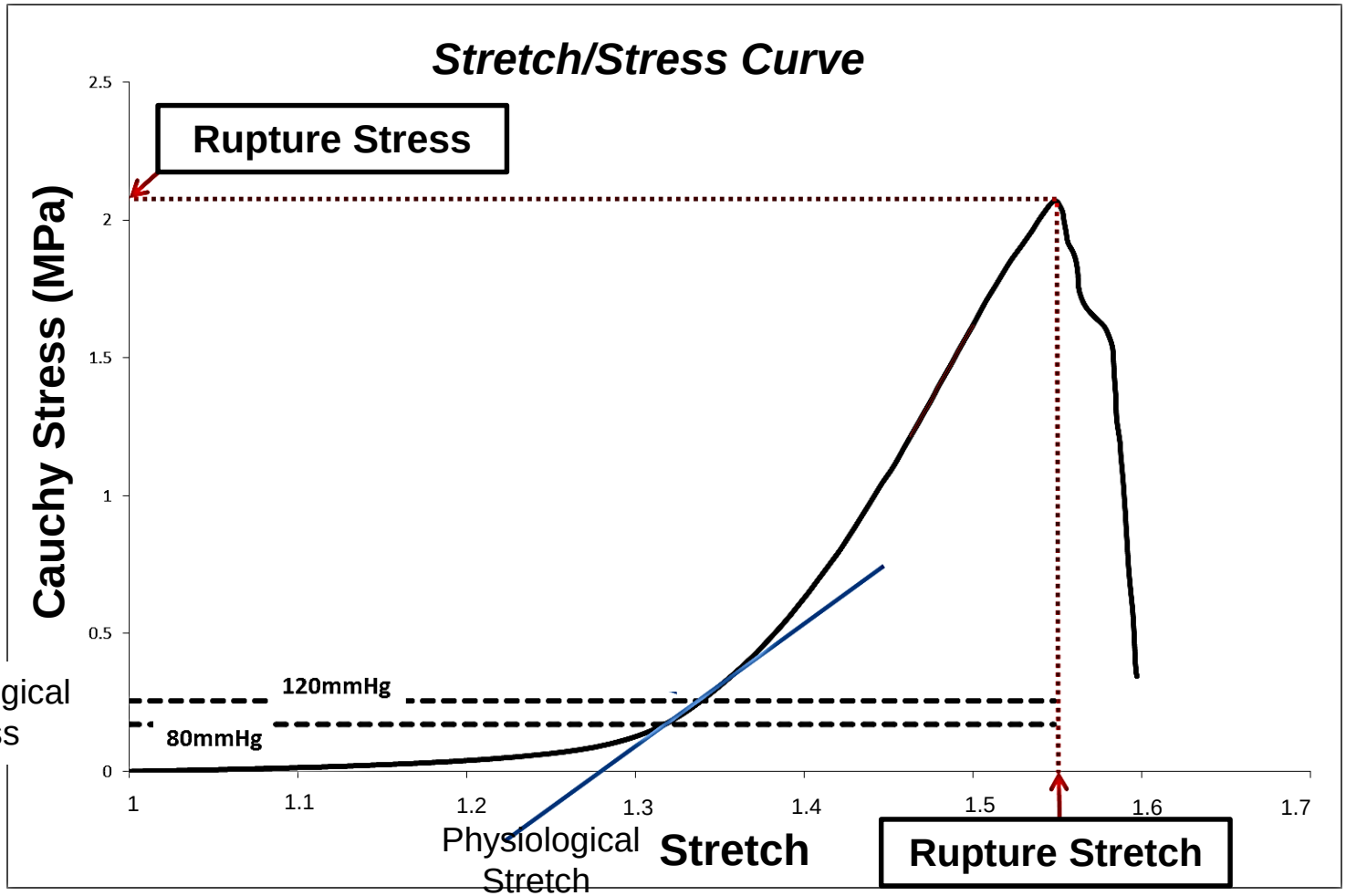

avril@emse.fr

Comparison with other studies

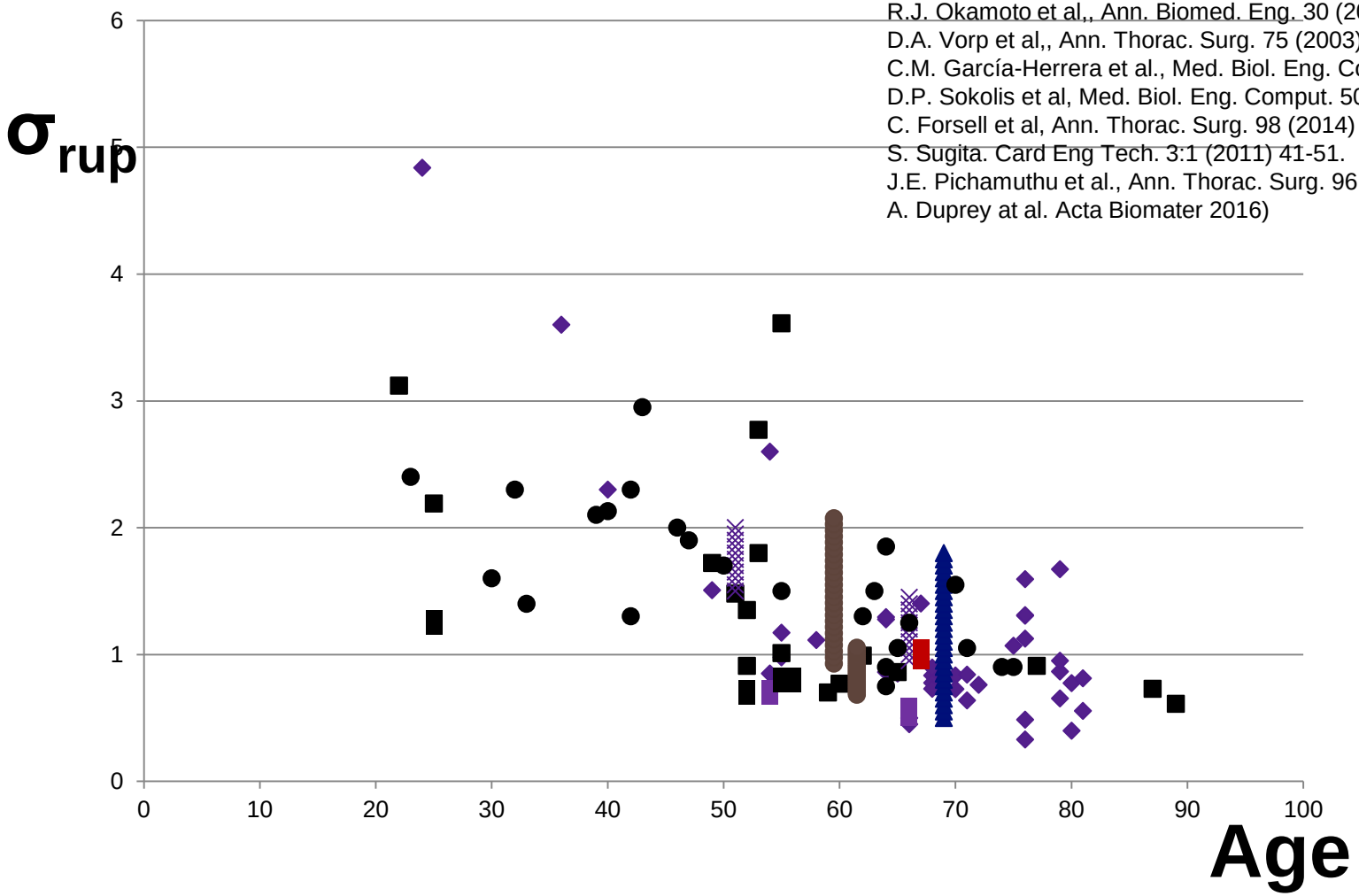

R.J. Okamoto et al,, Ann. Biomed. Eng. 30 (2002) 624–635.
D.A. Vorp et al,, Ann. Thorac. Surg. 75 (2003) 1210–1214.
C.M. García-Herrera et al., Med. Biol. Eng. Comput. 50 (2012) 559–566.
D.P. Sokolis et al, Med. Biol. Eng. Comput. 50 (2012) 1227–1237
C. Forsell et al, Ann. Thorac. Surg. 98 (2014) 65–71
S. Sugita. Card Eng Tech. 3:1 (2011) 41-51.
J.E. Pichamuthu et al., Ann. Thorac. Surg. 96 (2013) 2147–2154
A. Duprey at al. Acta Biomater 2016)

Comparison with other studies

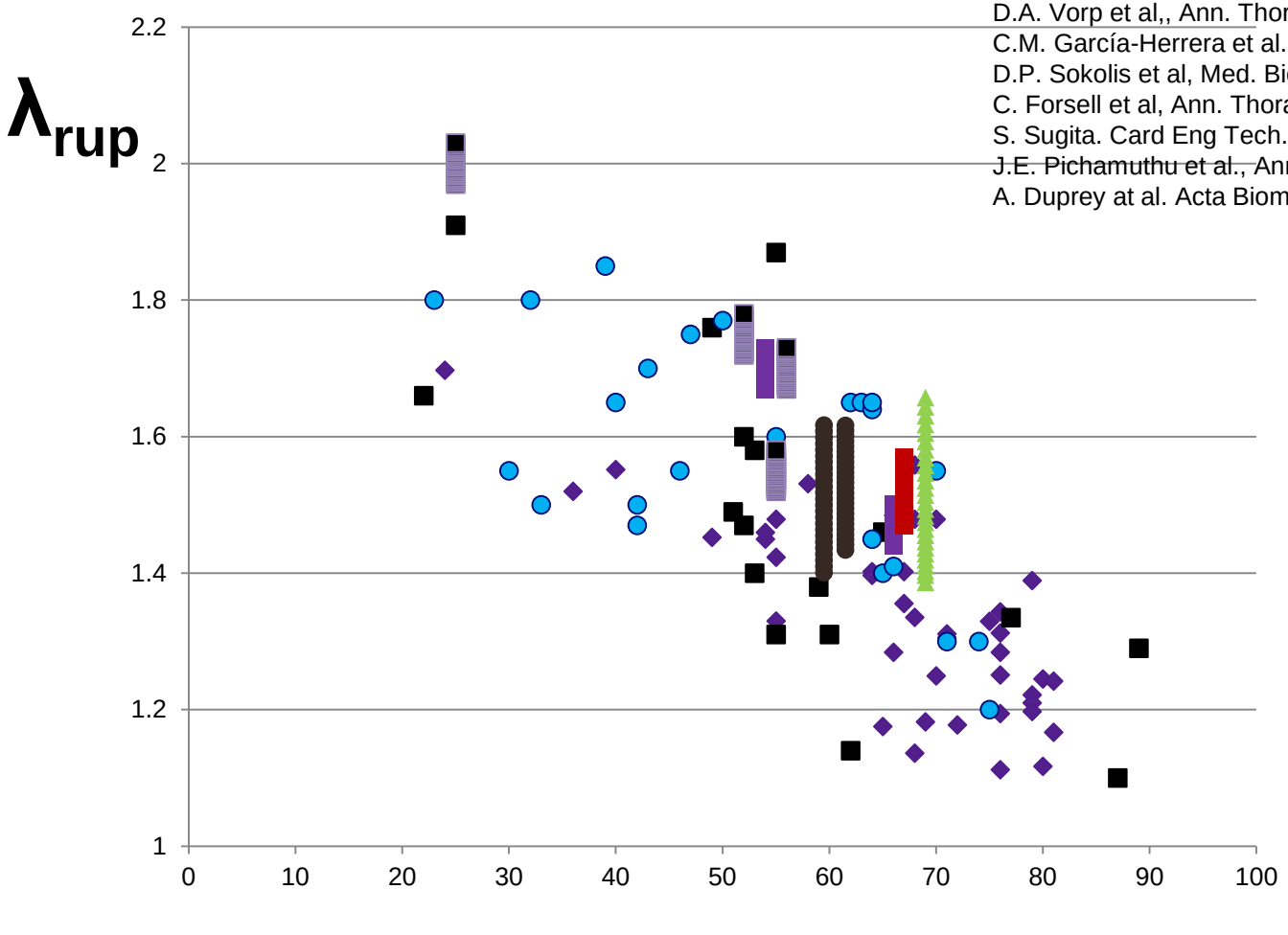

R.J. Okamoto et al,, Ann. Biomed. Eng. 30 (2002) 624–635.
D.A. Vorp et al,, Ann. Thorac. Surg. 75 (2003) 1210–1214.
C.M. García-Herrera et al., Med. Biol. Eng. Comput. 50 (2012) 559–566..
D.P. Sokolis et al, Med. Biol. Eng. Comput. 50 (2012) 1227–1237
C. Forsell et al, Ann. Thorac. Surg. 98 (2014) 65–71
S. Sugita. Card Eng Tech. 3:1 (2011) 41-51.
J.E. Pichamuthu et al., Ann. Thorac. Surg. 96 (2013) 2147–2154
A. Duprey at al. Acta Biomater 2016)

Rupture risk estimation

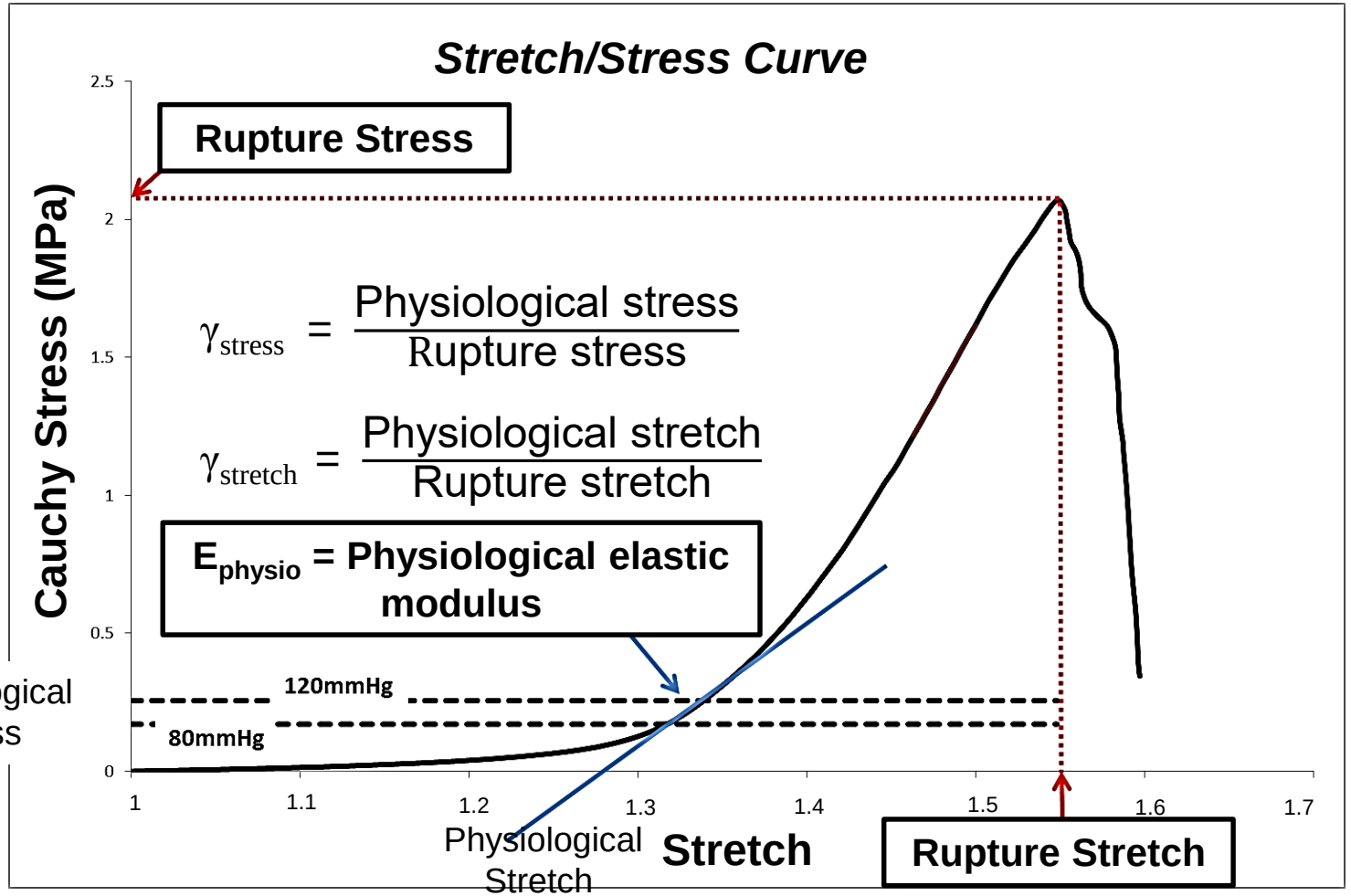

Correlation between $\gamma_{stretch}$ and E_{physio}

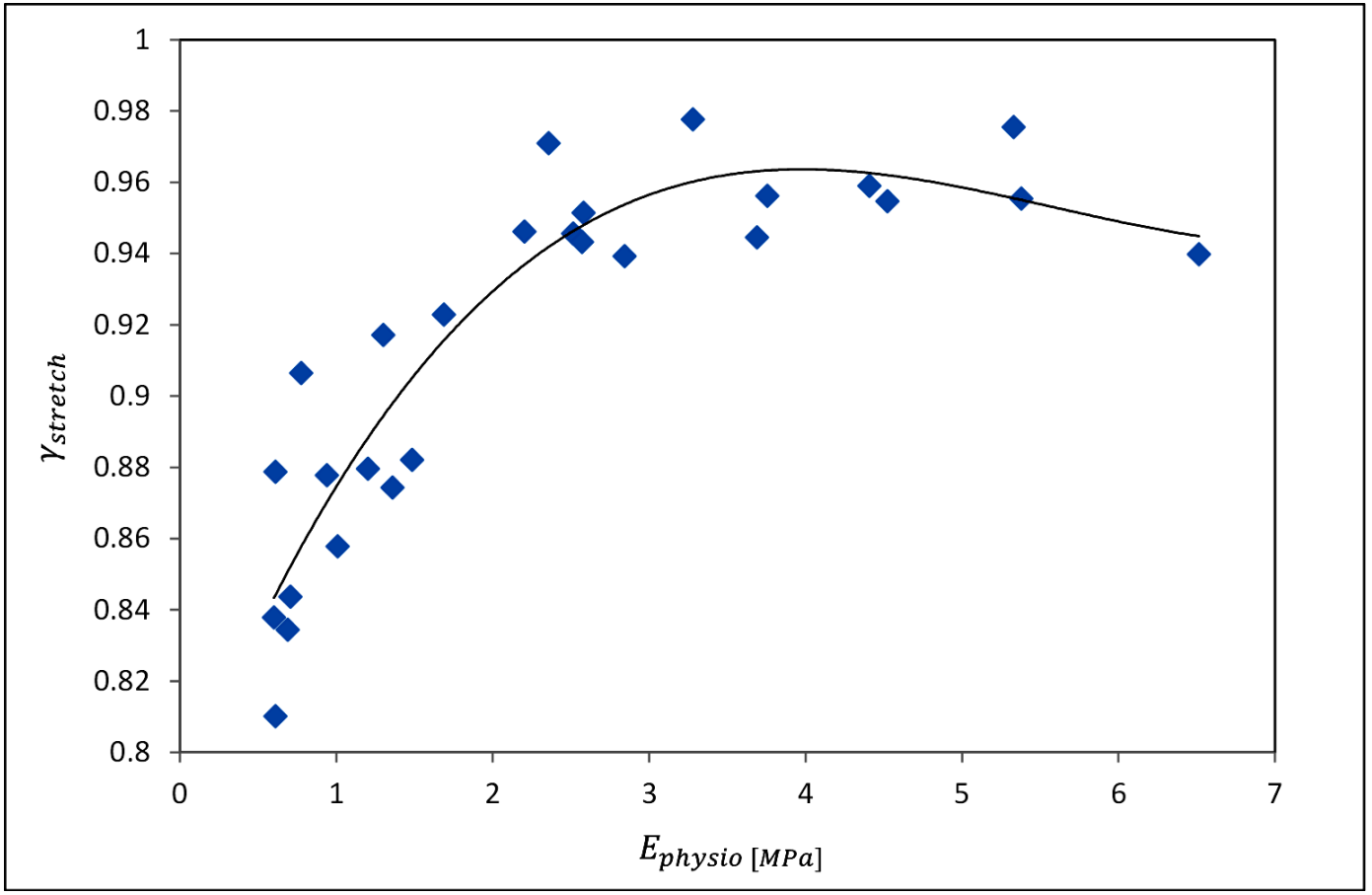

Duprey A, et al. Biaxial rupture properties of ascending thoracic aortic aneurysms. ***Acta Biomaterialia 2016.***

Distensibility measurements using the dynamic CT scan

- $D = (A_{max}-A_{min})/A_{min}/(P_{max}-P_{min})$
- $E_{physio} = 2R/Dh$

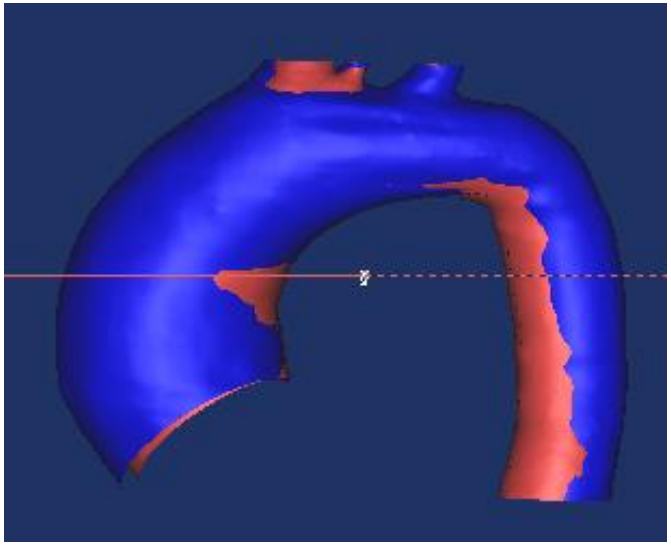

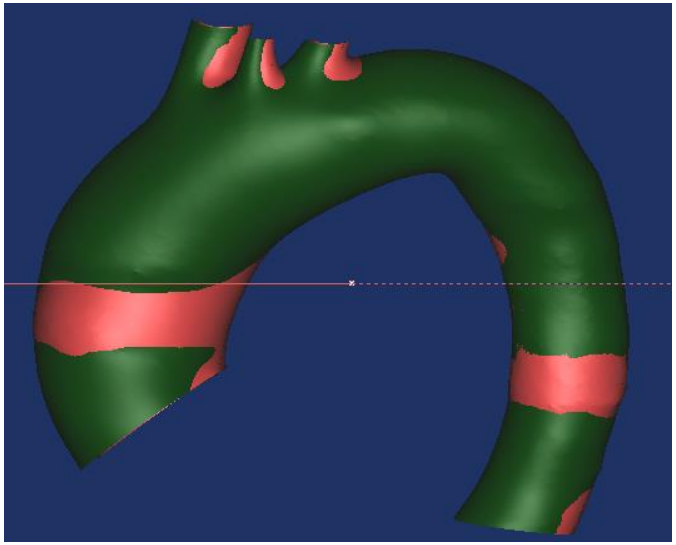

Correlation between $\gamma_{stretch}$ and E_{physio}

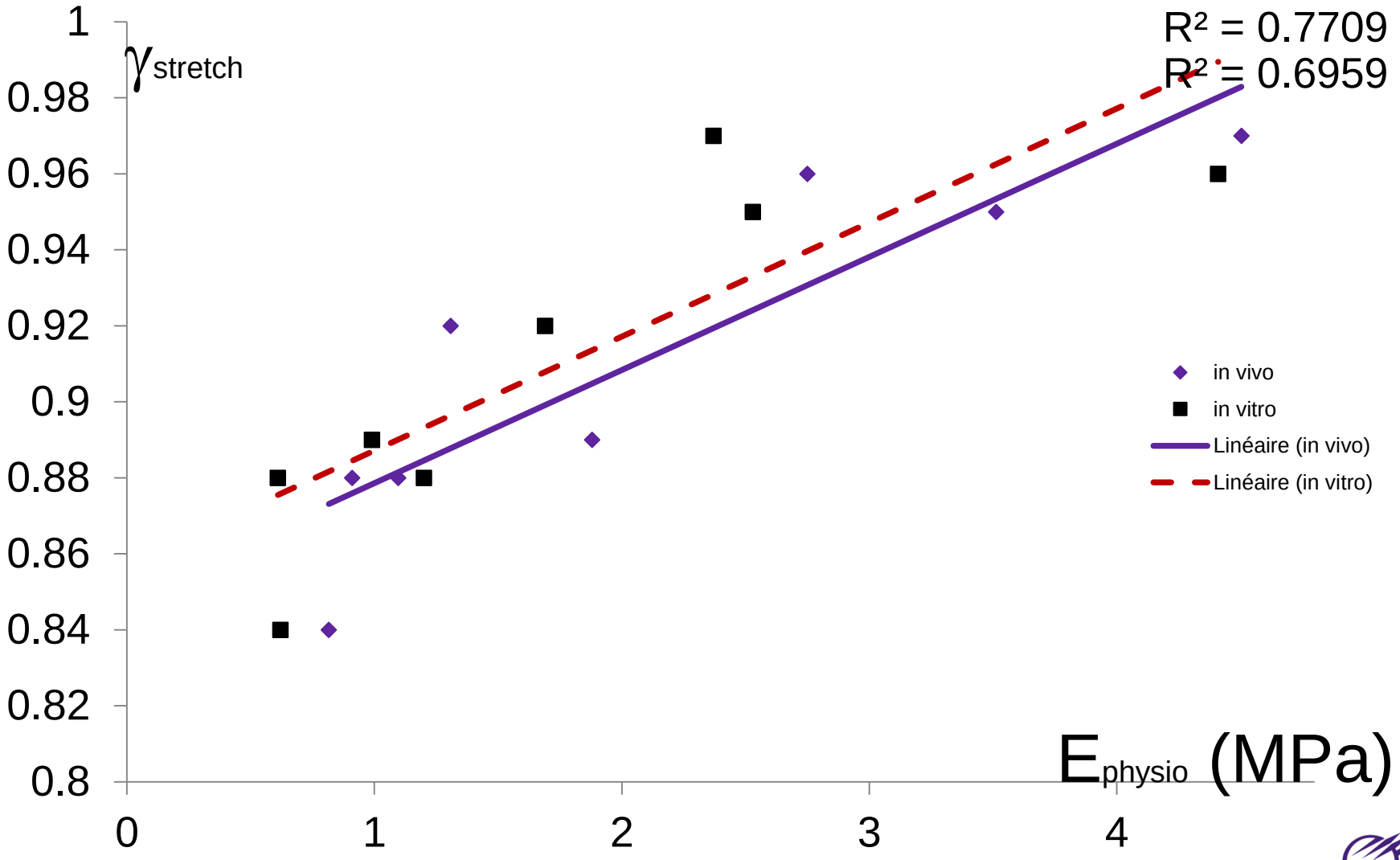

avril@emse.fr

Summary

- 2 ways of defining rupture:
  - PWS – but unknown patient-specific strength
  - $\gamma_{stretch}$ correlated with in vivo distensibility

Higher distensibility $\Rightarrow$ less risk because the aneurysm can more easily withstand volume variation

C. Martin et al., Acta Biomater. 9 (2013) 9392–9400

Future work

- **Extend the analysis to other patients**
- **Define a threshold for the new risk of rupture**
- **Predict the long-term evolution of this criterion for small aneurysms using mechanobiological models**

Histological interpretation

- **ATAA enlargement is a consequence of elastin damage**
- **More and more collagen tends to be recruited in the physiological range**

Patient with largest $\gamma_{stretch}$

Patient with smallest $\gamma_{stretch}$

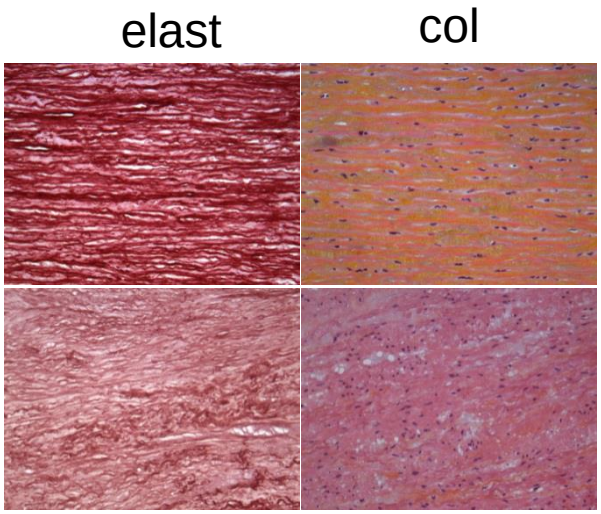

M.R. Hill et al,, J. Biomech. 45 (2012) 762–771

Computer fluid dynamics

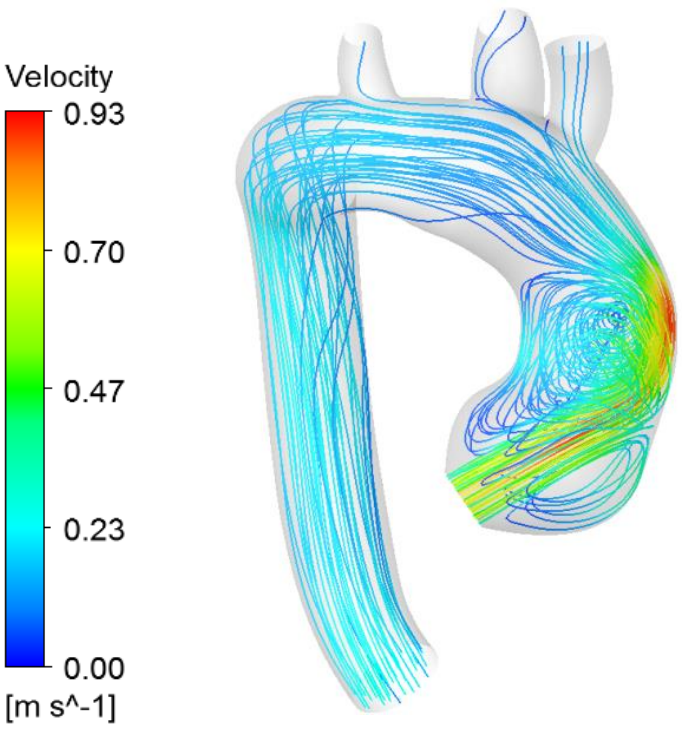

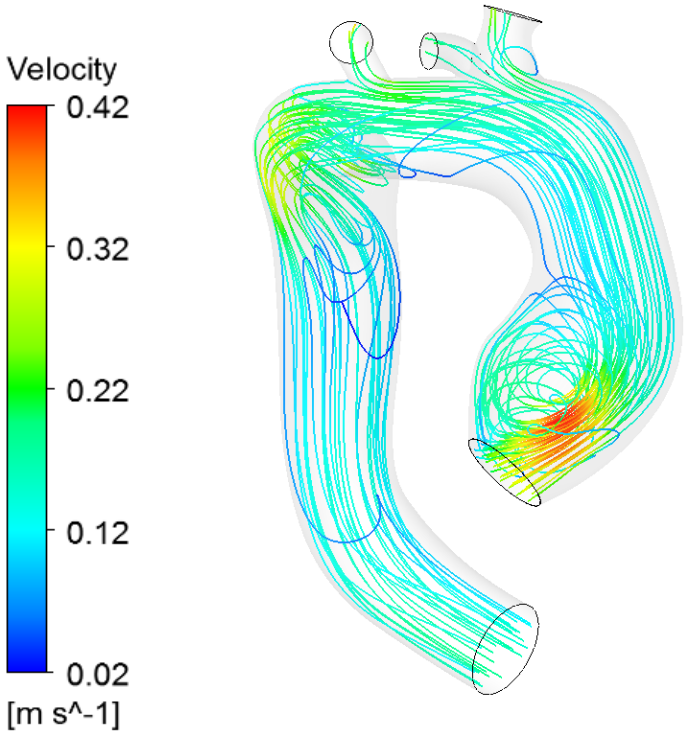

Acknowledgements

- **Olfa Trabelsi**
- **Ambroise Duprey**
- **Aaron Romo**
- **Pierre Badel**
- **Frances Davis**
- **Jean-Pierre Favre**
- **Victor Acosta**
- **Jamal Mousavi**
- **Solmaz Farzeneh**
- **Francesca Condemi**
- **Miguel Angel Gutierrez**
- **Oscar Alberto Mendoza**

Funding:

ERC-2014-CoG BIOLOCHANICS

European Research Council

CHU Saint-Étienne

MINES Saint-Étienne

UNIVERSITÉ DE LYON

LUX ET VERITAS

SAINBIOSE
SAnté INgéniérie BIOlogie Saint-Etienne
U1059 • INSERM • SAINT-ETIENNE

Inserm
Institut national de la santé et de la recherche médicale

Inverse characterization of regional, nonlinear and anisotropic properties of arteries

Matthew R MERSI, Chiara BELLINI, Paolo DI ACHILLE, Jay D HUMPHREY,

Prof Stéphane AVRIL (avril@emse.fr)

INSPIRING INNOVATION INNOVANTE PAR TRADITION

INTRODUCTION AND RATIONALE: EXAMPLE OF ATAA PHYSIOPATHOLOGY

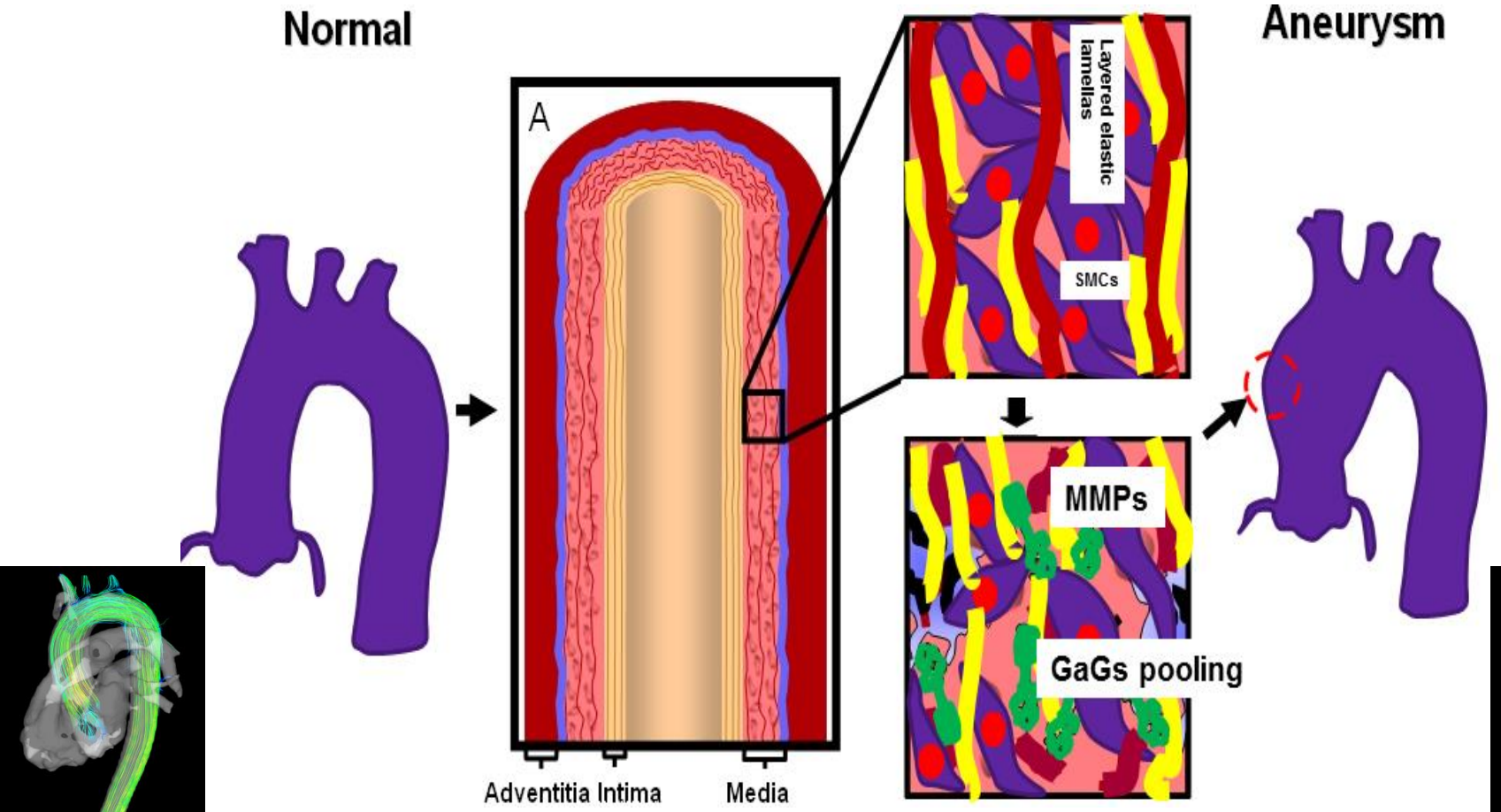

Laminar flow

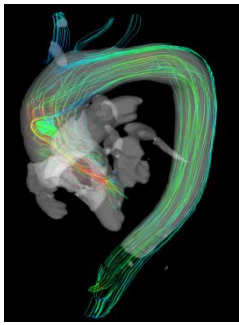

Disturbed hemodynamics

POINT OF VIEW OF MECHANOBIOLOGY

Altered mechanics induce biological responses, including gene expression, protein activation and cell phenotype

POINT OF VIEW OF BIOMECHANICS

Macroscopic manifestations ultimately dictate the mechanical functionality and structural integrity of the aortic wall

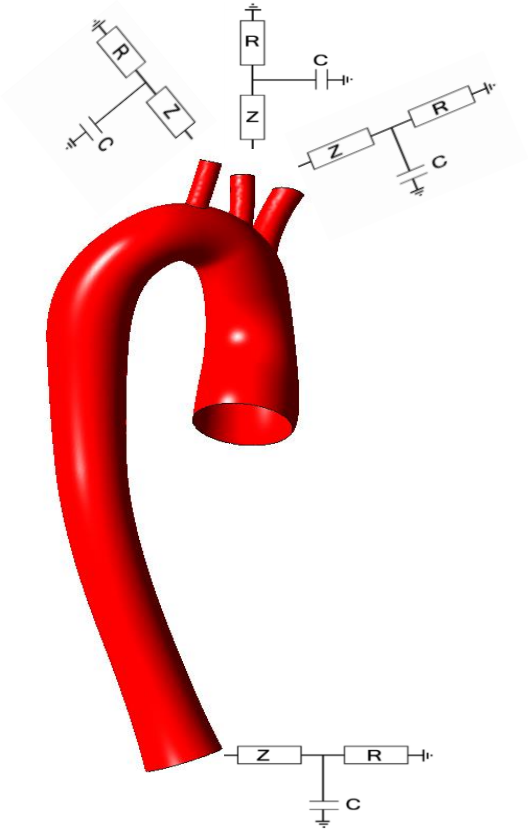

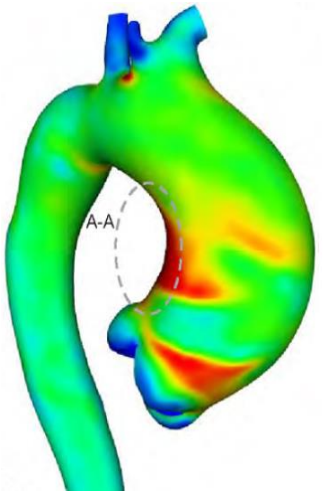

Martufi et al. Biomech. Model. Mechanobio. pp. 917–928, 2014.

CHALLENGES AND OBJECTIVES

Fundamentally understand local structure–function relationships in aortic aneurysms.

This requires an approach permitting:

1. **To reconstruct the regional distribution of mechanical properties of the aorta during aneurysm growth.**

2. **To investigate their correlation with the underlying microstructure and its evolutions.**

APPROACH

1. Experiments
2. Material model
3. Inverse method

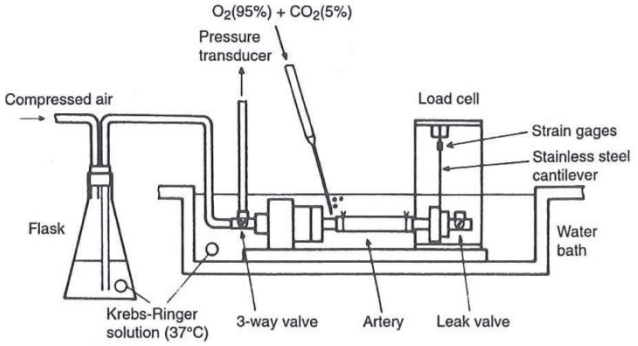

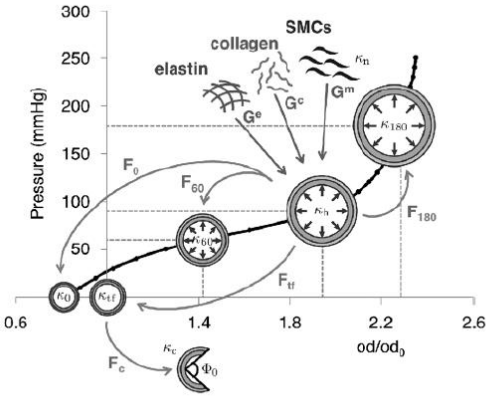

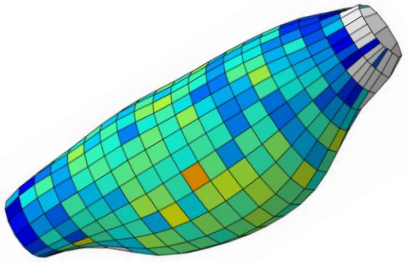

APPROACH

1. **Experiments**
2. Material model
3. Inverse method

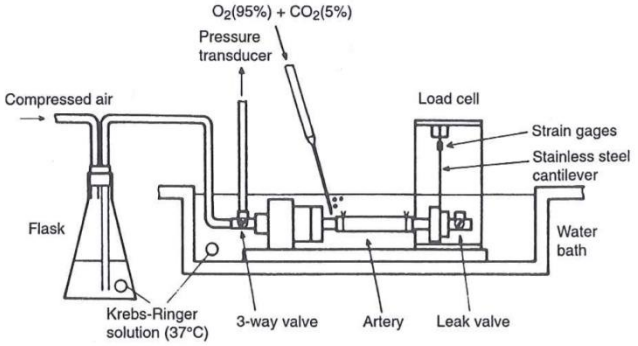

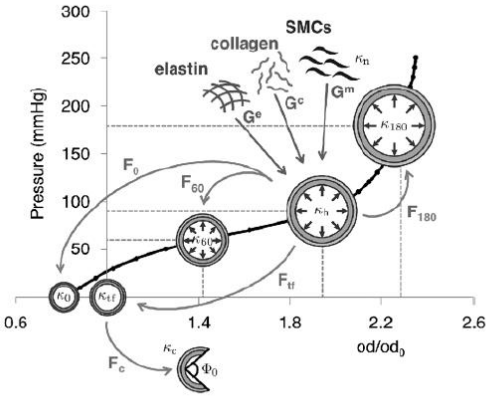

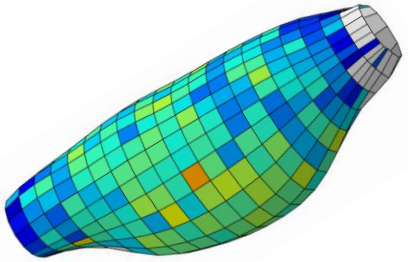

TENSION – INFLATION OF MICE AORTAS

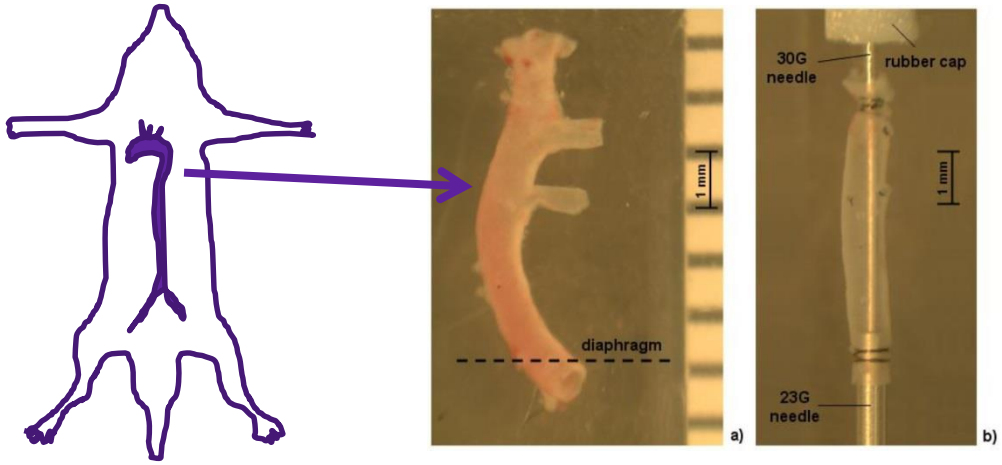

Gleason, et al. J. Biomech. Eng. **126**(6), p. 787, 2004.

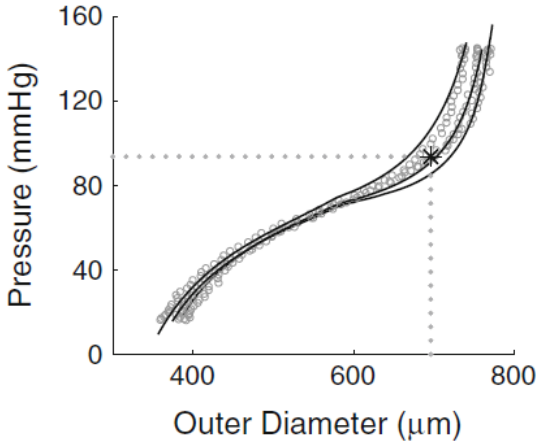

Humphrey , Cardiovascular Solid Mechanics, 2002

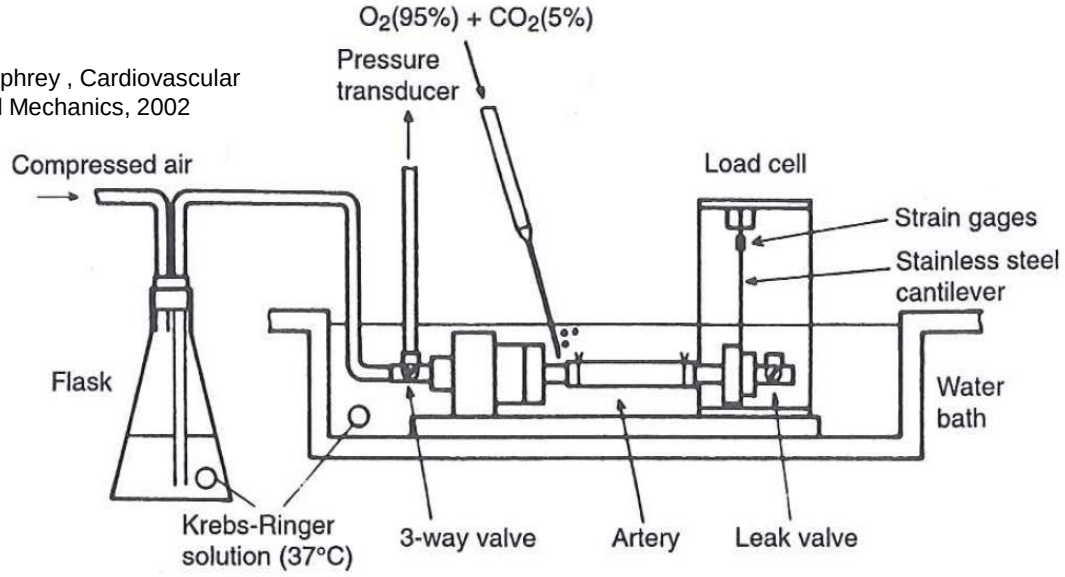

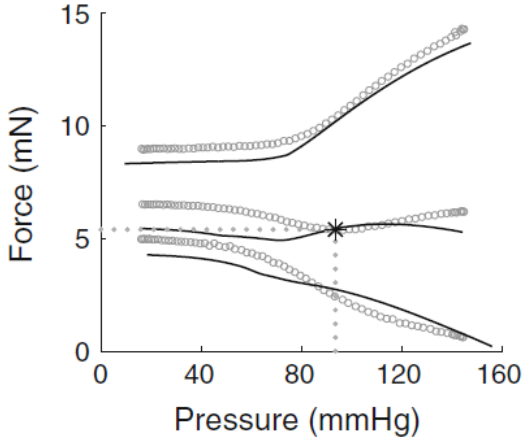

MEASUREMENT OF THE RESPONSE USING DIGITAL IMAGE CORRELATION

classical

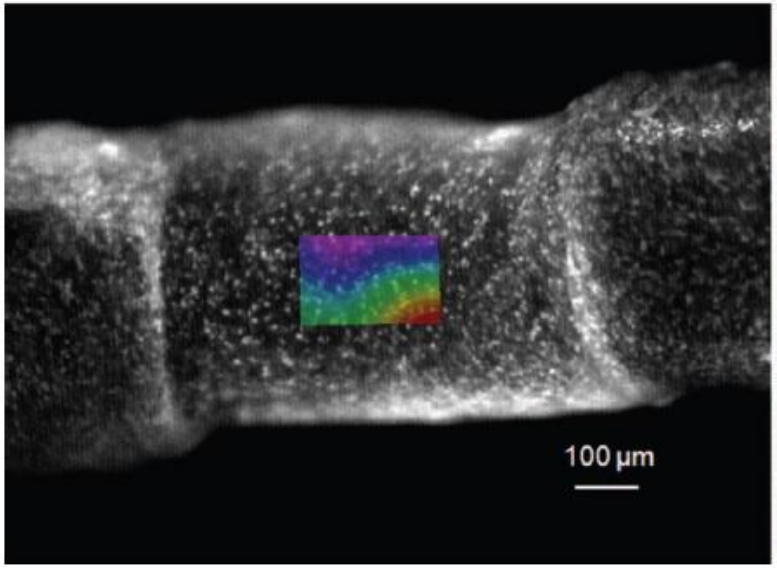

Badel et al. CMBBE, **15**, p 37-48, 2012.

panoramic

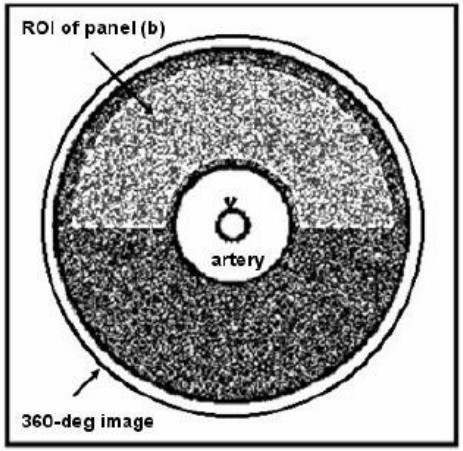

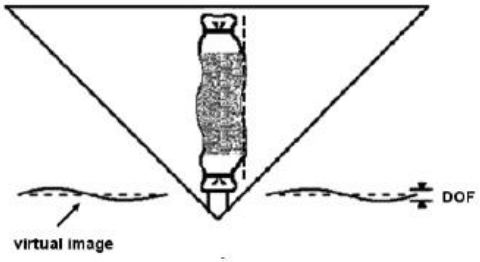

Genovese. Optics Lasers Eng, **47**, p 995-1008, 2009.

PANORAMIC DIGITAL IMAGE CORRELATION - pDIC

Genovese et al, CMBBE, **14**, p. 213-237, 2011.

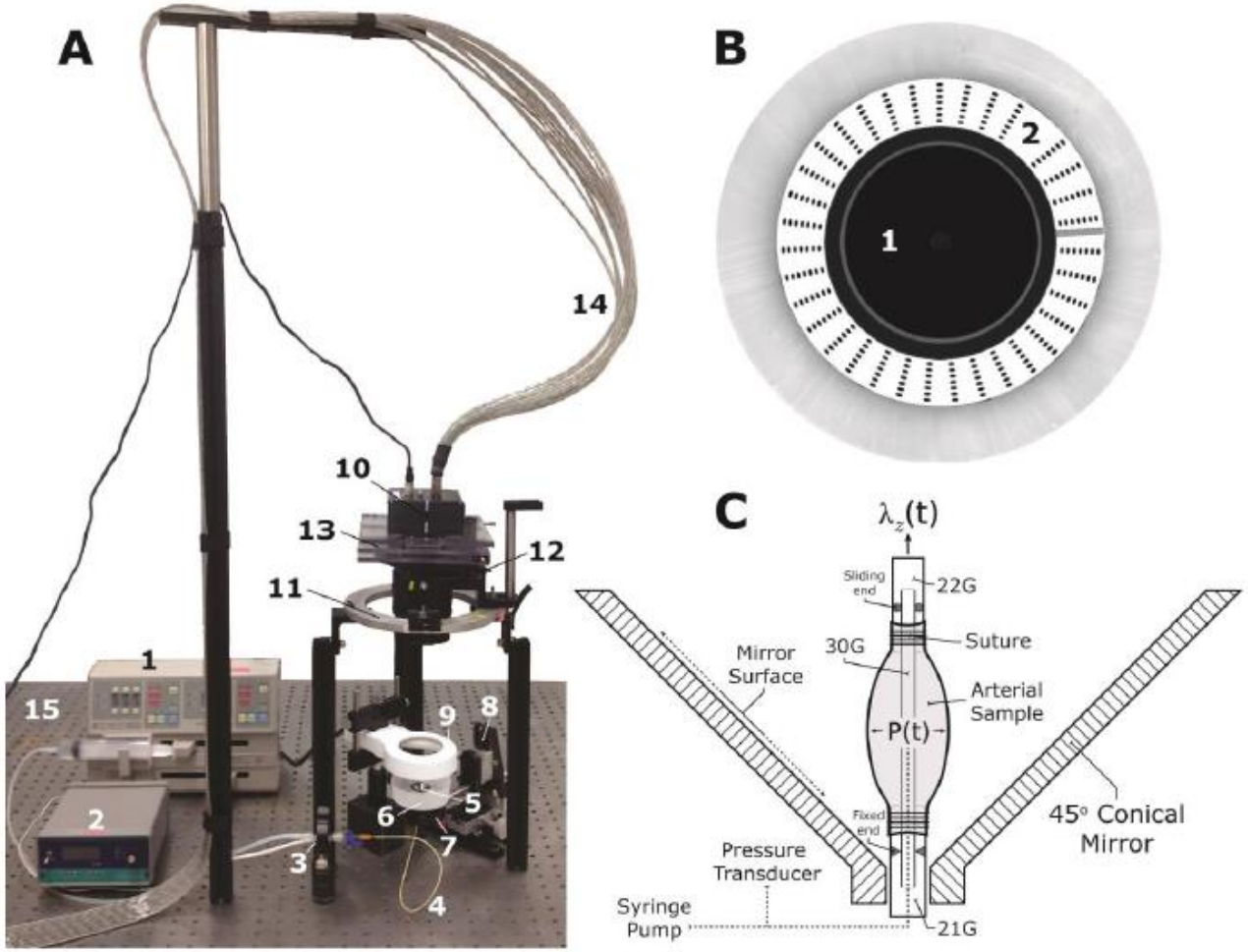

avril@emse.fr

Full-field strain measurement across the outer surface of the artery

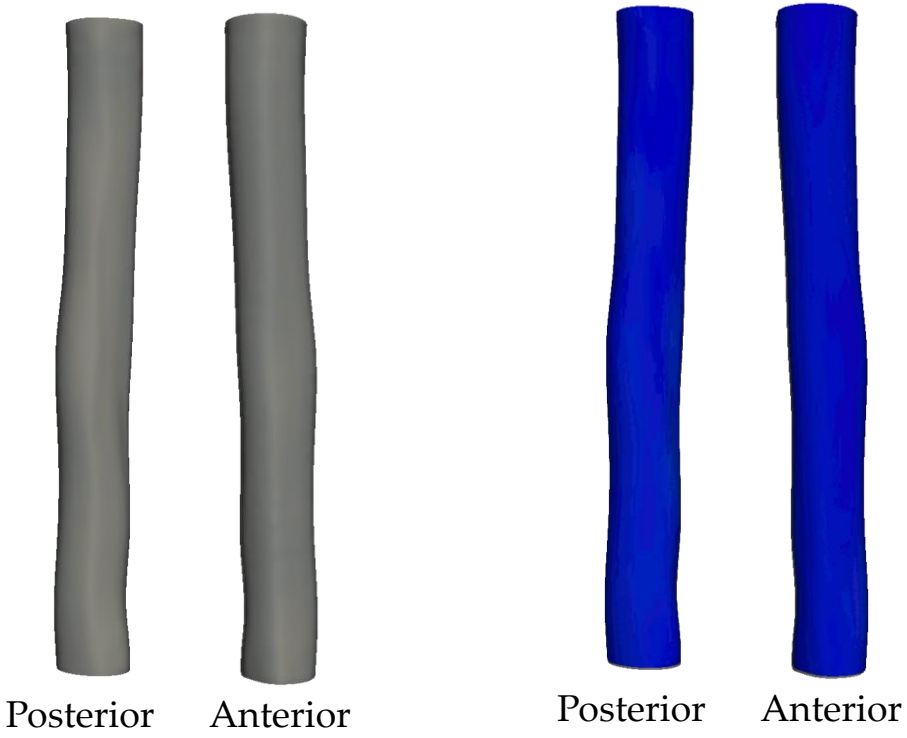

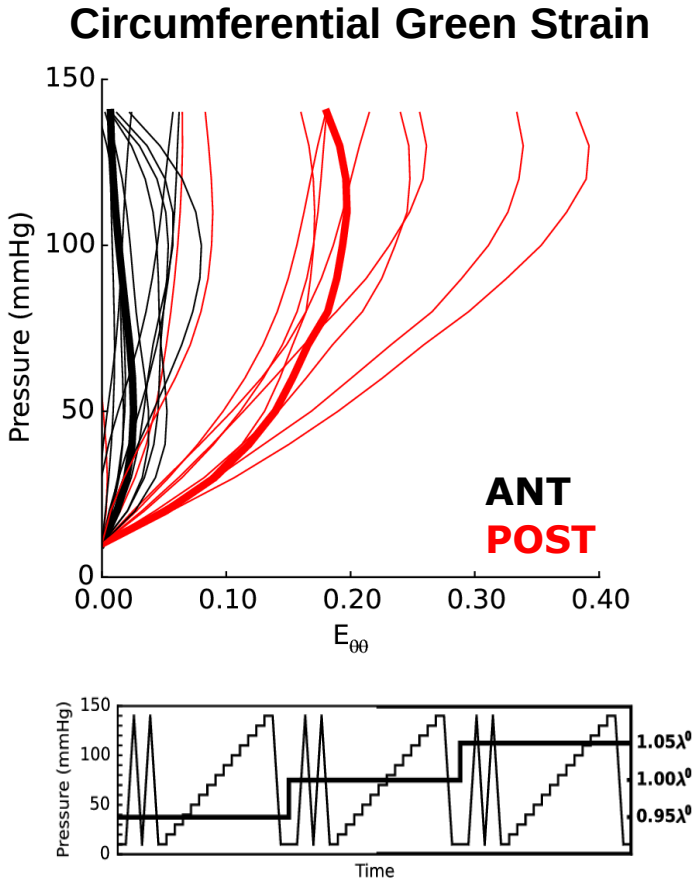

avril@emse.fr

APPROACH

1. Experiments
2. **Material model**
3. Inverse method

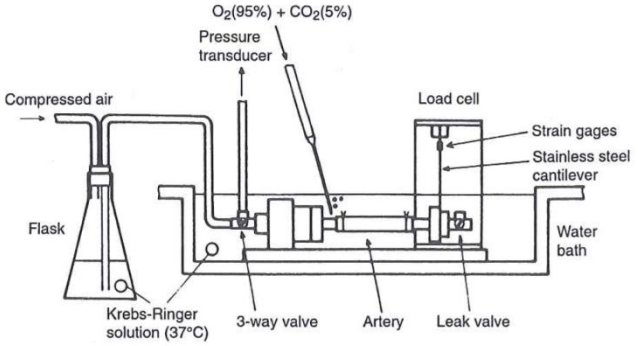

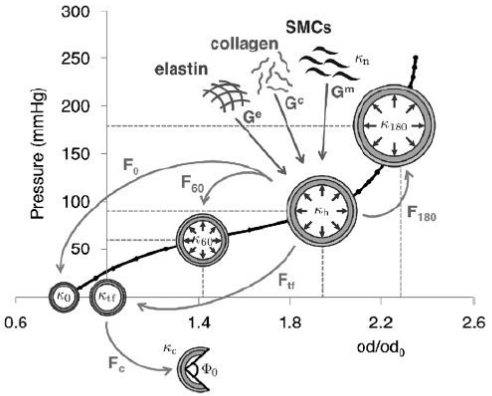

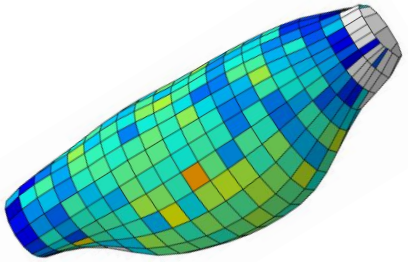

CONSTITUTIVE MODEL

Strain energy functions:

$$W = \phi^{e} W^{e}(\mathbf{F}^{e}) + \phi^{m} W^{m}(\lambda^{m}) + \sum_{j=1}^{4} \phi^{c_j} W^{c_j}(\lambda^{c_j})$$

$$W^{e}(\mathbf{F}^{e}) = \frac{c^{e}}{2}\left[\mathrm{tr}\left((\mathbf{F}^{e})^{T}\mathbf{F}^{e}\right) - 3\right]$$

$$W^{m}(\lambda^{m}) = \frac{c_2^{m}}{4c_3^{m}}\left[e^{c_3^{m}\left((\lambda^{m})^2-1\right)^2} - 1\right]$$

$$W^{c}(\lambda^{c_j}) = \frac{c_2^{c}}{4c_3^{c}}\left[e^{c_3^{c}\left((\lambda^{c_j})^2-1\right)^2} - 1\right]$$

Bellini, et al., Ann. Biomed. Eng., **42**(3), pp. 488–502, 2014

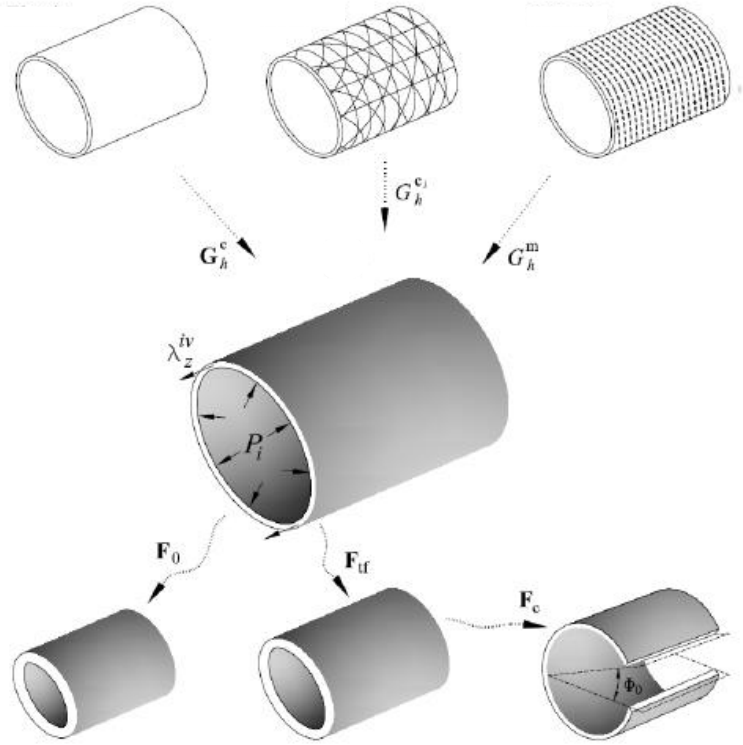

CONSTITUTIVE MODEL

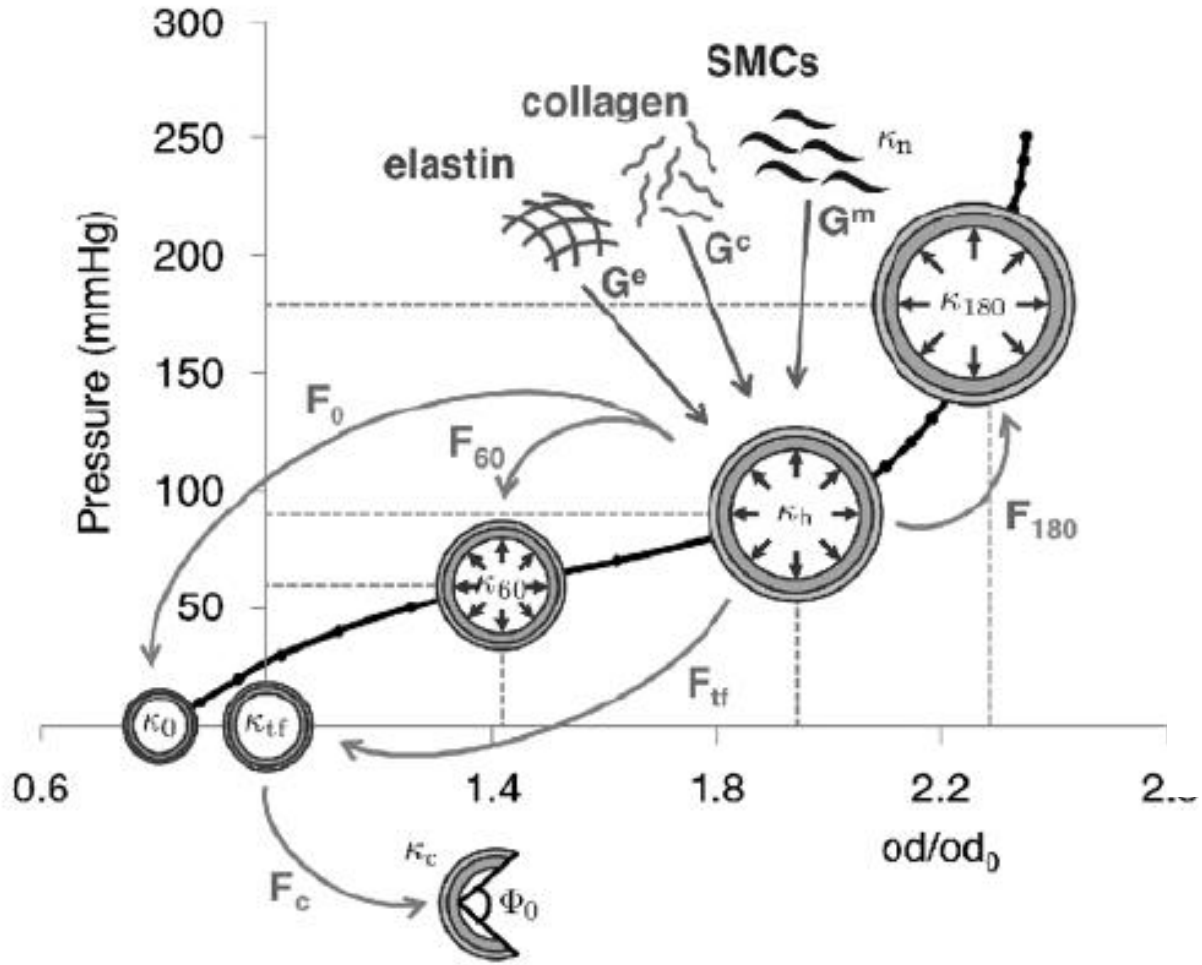

FE implementation

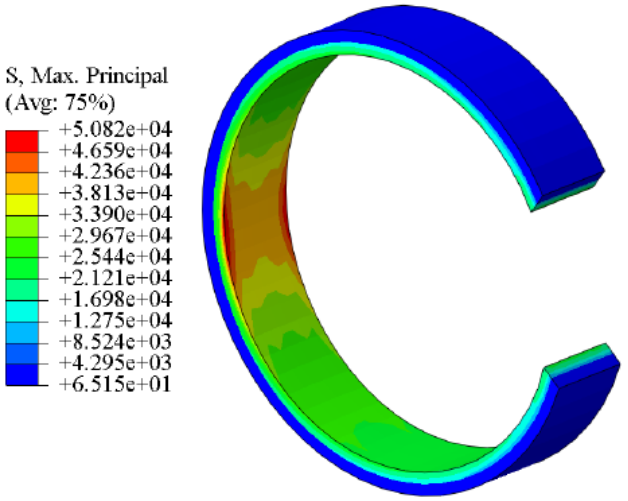

Bellini, et al., Ann. Biomed. Eng., **42**(3), pp. 488–502, 2014

PARAMETERS TO BE IDENTIFIED

$$W = \phi^{e} W^{e}(\mathbf{F}^{e}) + \phi^{m} W^{m}(\lambda^{m}) + \sum_{j=1}^{4} \phi^{c_j} W^{c_j}(\lambda^{c_j})$$

$$W^{e}(\mathbf{F}^{e}) = \frac{c^{e}}{2}\left[\mathrm{tr}\left((\mathbf{F}^{e})^{T}\mathbf{F}^{e}\right) - 3\right]$$

$$W^{m}(\lambda^{m}) = \frac{c_2^{m}}{4c_3^{m}}\left[e^{c_3^{m}(\lambda^{m})^2-1)^2} - 1\right]$$

$$W^{c}(\lambda^{c_j}) = \frac{c_2^{c}}{4c_3^{c}}\left[e^{c_3^{c}(\lambda^{c_j})^2-1)^2} - 1\right]$$

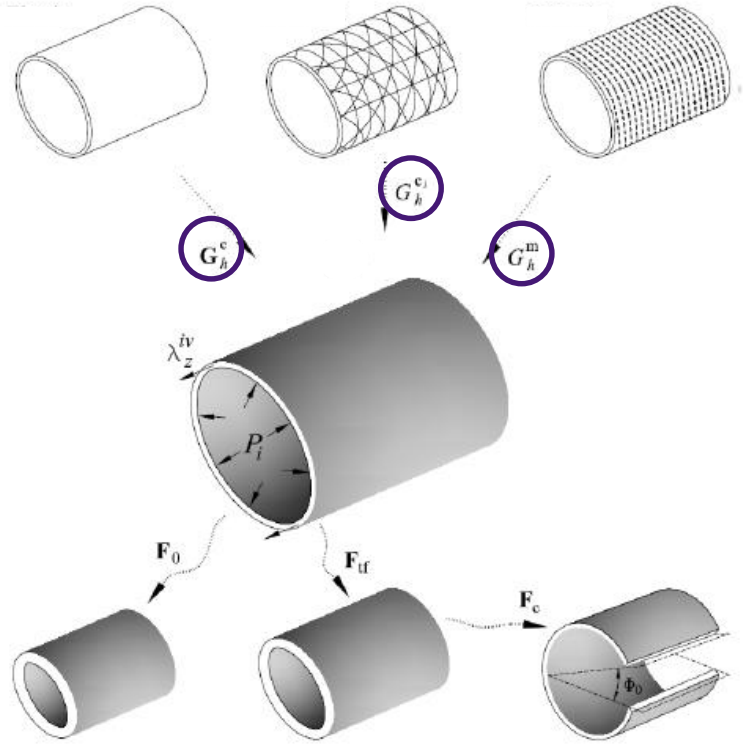

APPROACH

1. Experiments
2. Material model
3. **Inverse method**

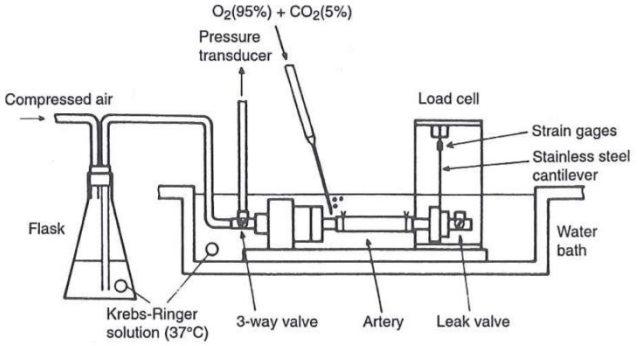

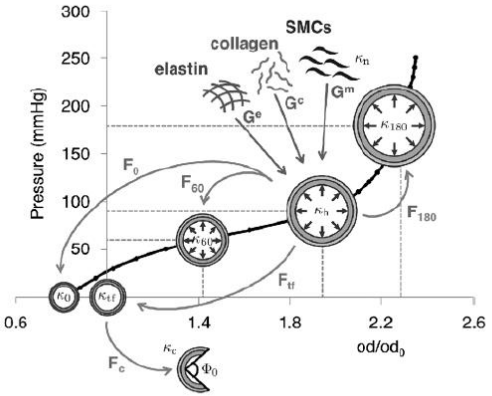

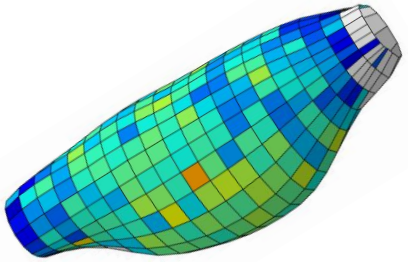

Inverse approach – traditional approach

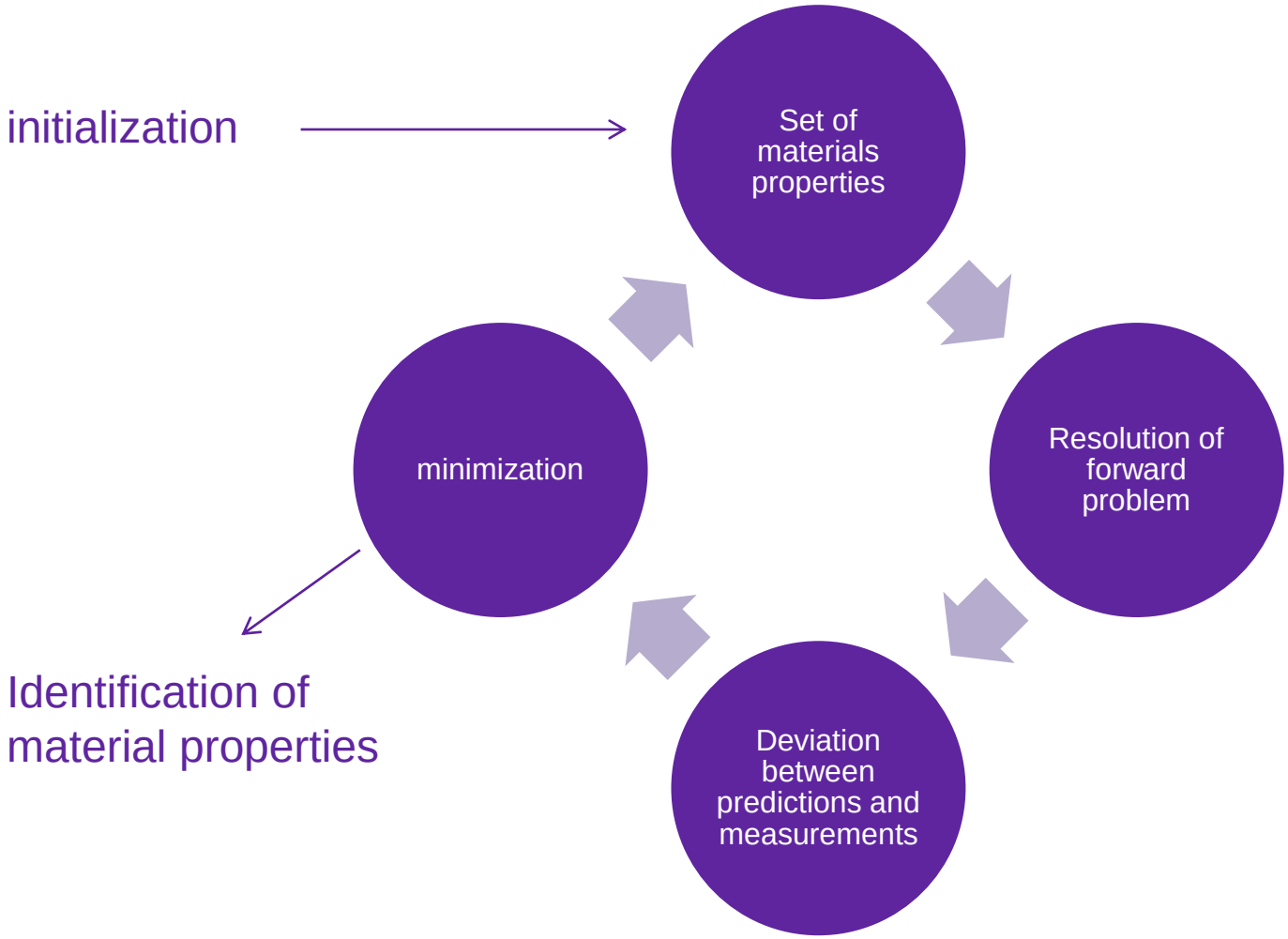

The virtual fields method

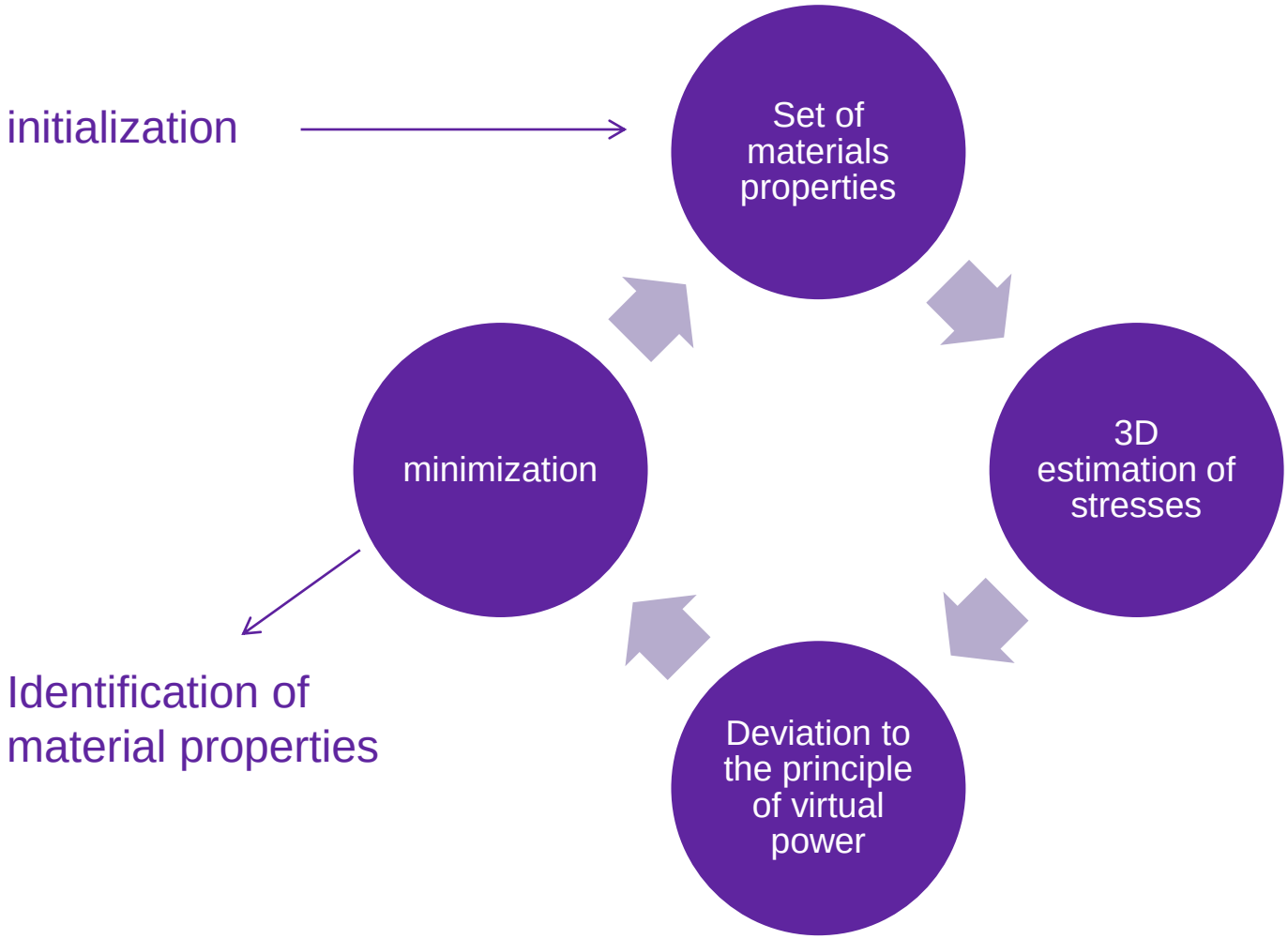

Results

Control

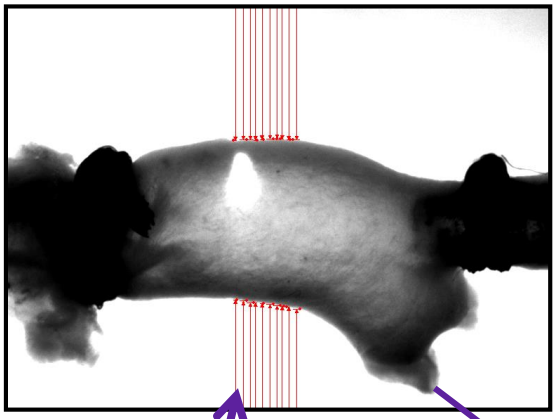

Fibulin 4 SMC KO

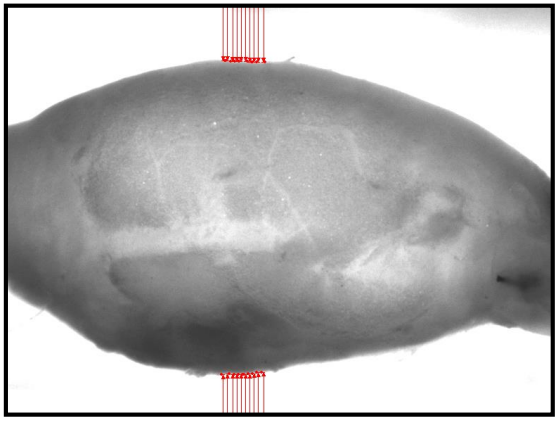

Fibrillin 1 *mgR/mgR*

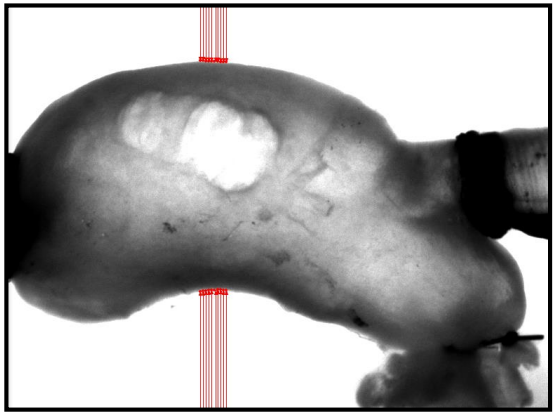

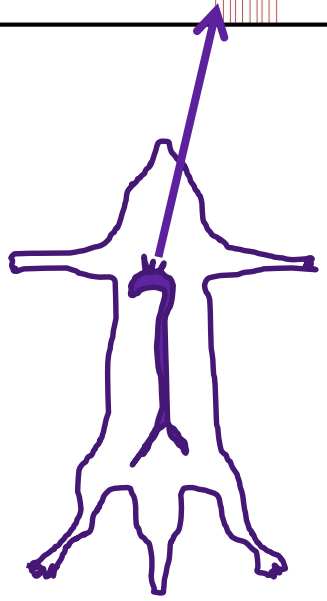

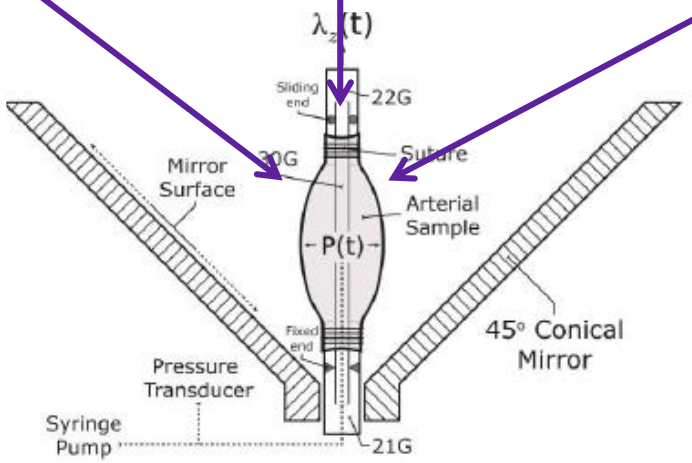

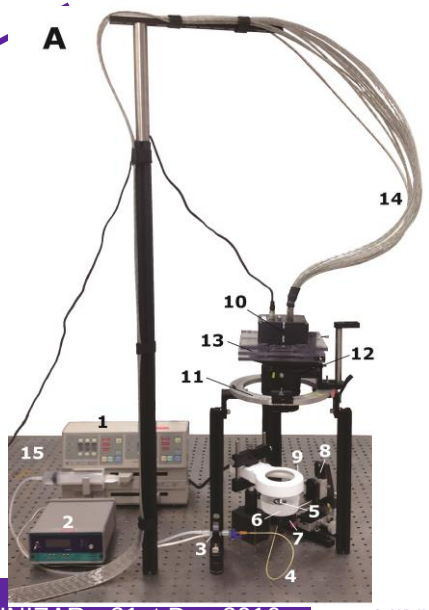

pDIC measurements

Fibulin 4 SMC KO

ventral *dorsal* *inflation*

6852

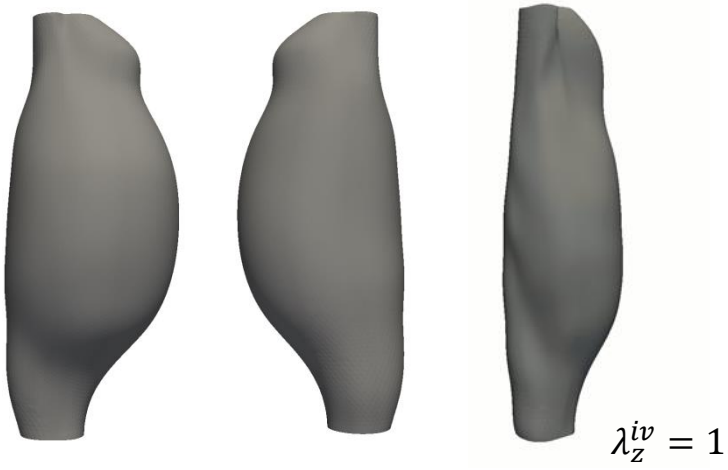

$\lambda_z^{iv} = 1.31$

$OD_{max} = 3.62$ mm

Fibrillin 1 *mgR/mgR*

ventral *dorsal* *inflation*

CS38

$\lambda_z^{iv} = 1.43$

$OD_{max} = 2.93$ mm

avril@emse.fr

Full-Field Material Parameter Estimation

- Circumferential linearized stiffness (@ λ_z^{iv} and 100 mmHg)

Fibulin 4 SMC KO

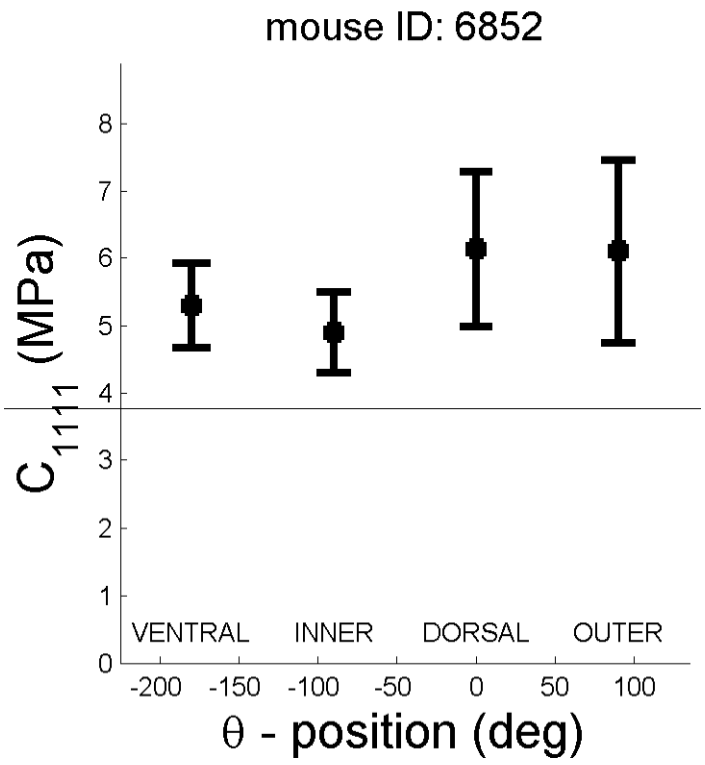

Fibrillin 1 *mgR/mgR*

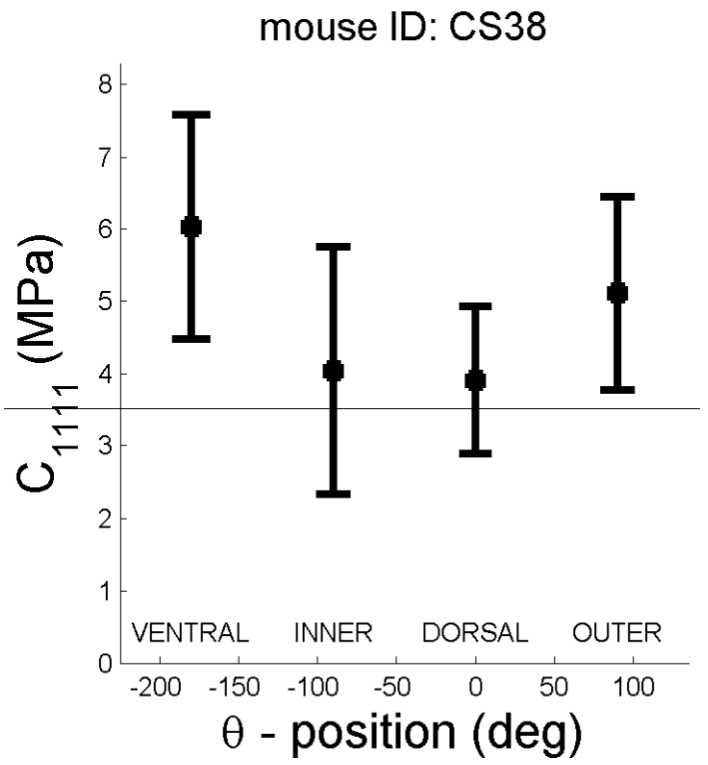

avril@emse.fr

Heterogeneity of the strain energy

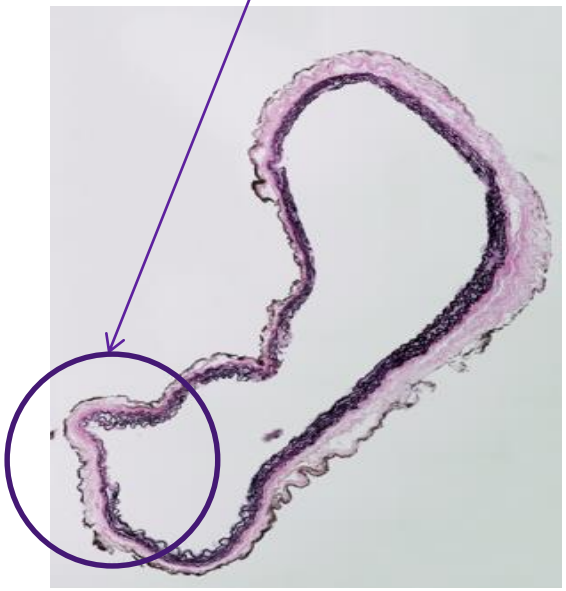

Fibrillin 1 *mgR/mgR*

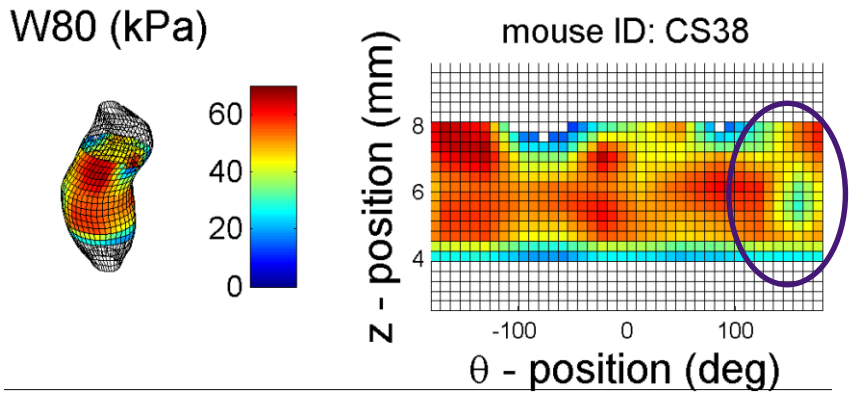

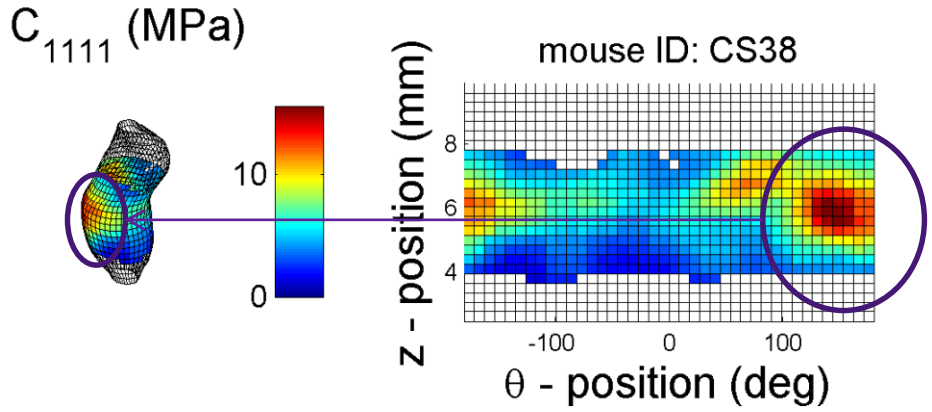

FUTURE WORK

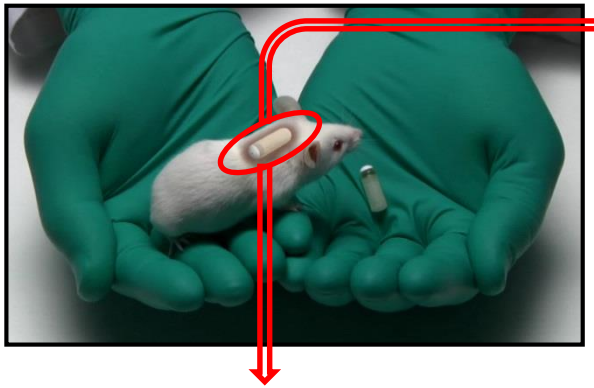

Dissecting Aortic Aneurysm

Aortic Dissection

Descending Thoracic

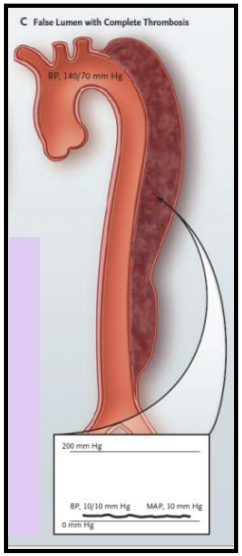

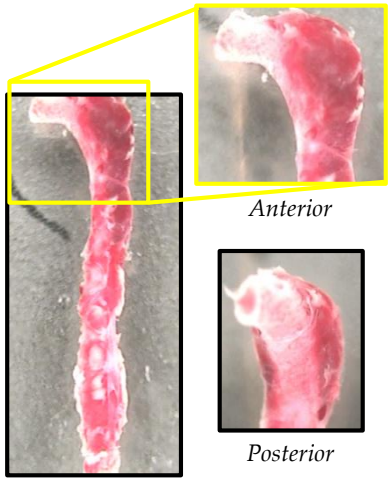

Suprarenal

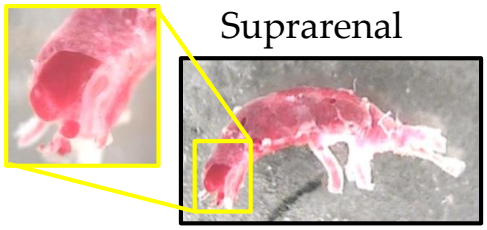

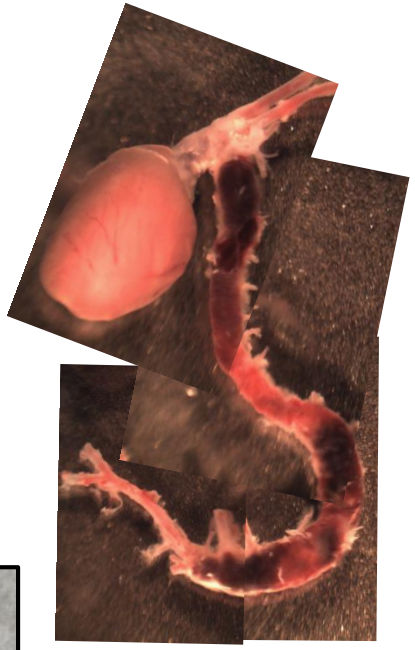

Intact Aorta

FUTURE WORK

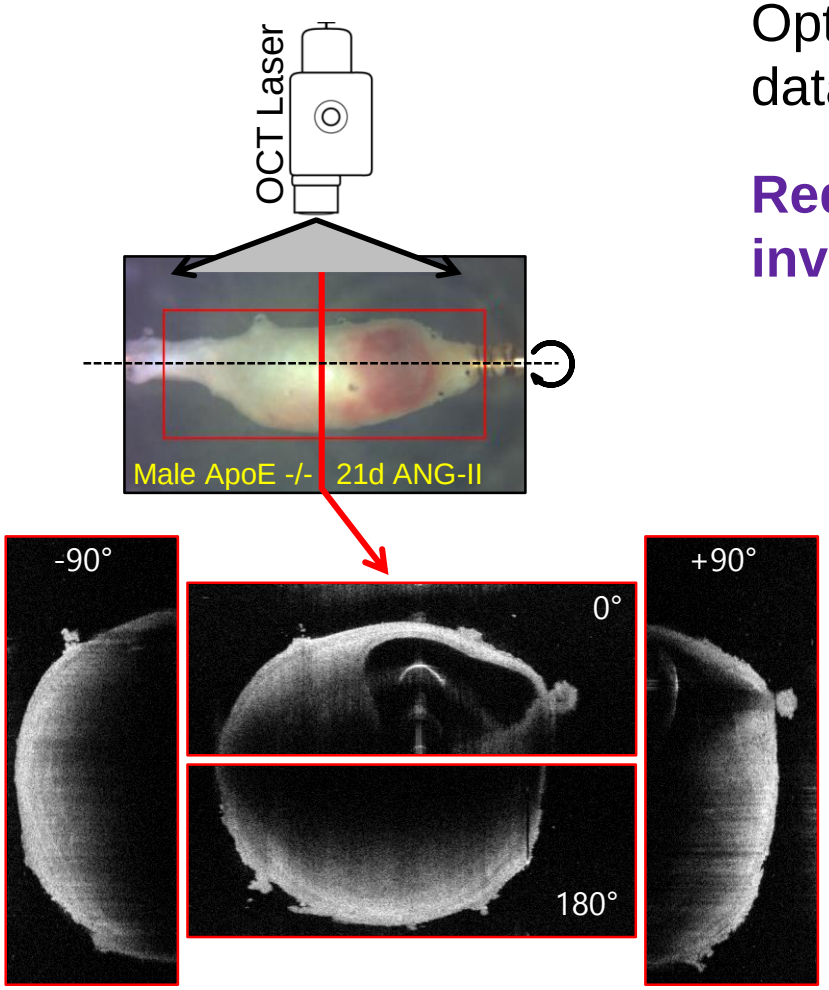

Optical Coherence Tomography (OCT) data are available from the experiments

Requires further developments of the inverse approach to be employed

Merged Cross-Section

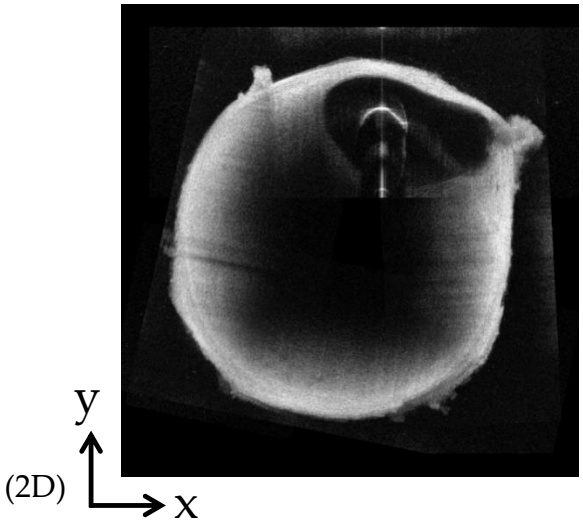

Acknowledgements

- **Matthew R Bersi**
- **Chiara Bellini**
- **Paolo Di Achille**
- **Jay D Humphrey**
- **Katia Genovese**

Funding:
NIH grants: R01 HL086418, R01 HL105297, U01 HL116323

ERC-2014-CoG BIOLOCHANICS

European Research Council